Renewable and Sustainable Energy Reviews 15 (2011) 3278–3300

Contents lists available at ScienceDirect

Renewable and Sustainable Energy Reviews

journal homepage: www.elsevier.com/locate/rser

Particulate emissions from biodiesel vs diesel fuelled compression ignition engine

Avinash Kumar Agarwal [a,*], Tarun Gupta [b], Abhishek Kothari [a]

[a] Department of Mechanical Engineering, Indian Institute of Technology Kanpur, Kanpur 208016, India
[b] Department of Civil Engineering, Indian Institute of Technology Kanpur, Kanpur 208016, India

ARTICLE INFO

Article history:
Received 14 May 2010
Accepted 20 January 2011

Keywords:
Particulate
Biodiesel
Heavy metals
Benzene soluble organic fraction
Morphology
Elemental composition

ABSTRACT

Studies conducted over the last decade have well established a direct relationship between deteriorating human health and diesel engine exhaust. Biodiesel has shown a lot of promise in terms of both its relatively higher combustion efficiency and lower harmful emissions. Biodiesel has the potential to replace a significant amount of the petroleum used to power diesel engines. The emissions from biodiesel are different than petroleum-based diesel and it is important to understand how they are different with respect to the levels emitted and the combustibility of the particulates. One of the major pollutants emitted from engine exhaust is particulate matter (PM). PM emitted from tailpipes contains a variety of toxic contaminants either embedded or adsorbed on its surface. This study provides a one to one comparison between PM emitted from a mid-size engine running on petroleum-based diesel versus biodiesel. The key physical and chemical parameters analyzed include metals, benzene soluble organic fraction, elemental and organic carbon fractions, particle morphology, particle number and size distribution. This is the first study of its kind where various aspects of the PM emitted from a biodiesel-operated engine have been extensively studied. The major results from the study showed that metals that come from engine wear are not present in biodiesel exhaust particulate due to its self lubricating properties. Samples collected of mineral diesel exhaust are relatively darker in color and stickier than biodiesel exhaust. Biodiesel and its blends gave more benzene soluble organic fraction (BSOF) in engine exhaust particulate matter than mineral diesel at all operating conditions. B100 gave higher number of smaller particles in its exhaust than mineral diesel; comprehensively all size particles were also higher in case of B100. Peak particle concentrations for biodiesel were shifted towards smaller size particles. As load increases, B20 emission performance in terms of particle concentrations improves very rapidly and even surpasses mineral diesel emission performance. Scanning electron microscope (SEM) images for B100 and B20 showed granular structure particulates with bigger grain size compared to mineral diesel. Among B100, B20 and mineral diesel, total particle accumulation was maximum for mineral diesel.

Contents

* Corresponding author. Tel.: +91 512 259 7982; fax: +91 512 259 7408.
E-mail address: akag@iitk.ac.in (A.K. Agarwal).

1364-0321/$ – see front matter © 2011 Elsevier Ltd. All rights reserved.
doi:10.1016/j.rser.2011.04.002

1. Introduction

The main concerns about particulates are environmental impact, adverse health effects, decreased visibility, and soiling of buildings. A strong relationship between exposure to vehicle-related air pollutant emissions and adverse human health impacts is now well established [1–3]. Diesel is the source of toxic species such as benzene and polycyclic aromatic hydrocarbons (PAH's), and metals in addition to the oxides of nitrogen (NO_x), and PM. Particulate mass is the only criteria applied by the automotive regulatory authorities all over the world even though all respiratory problems and toxicology related problems directly depend upon the particulate size and/or surface area.

Various health effects of particulates, from less serious to very serious ones are associated with its specific chemical and physical (but mostly chemical) components [4]. Exposure to heavy metals cause adverse health effects including toxicity [5]. Many organic pollutants such as polycyclic aromatic hydrocarbons (PAH's) are carcinogenic, mutagenic and genetotoxic, even if they are present in small concentrations. Therefore, it is important to identify potential sources and characterize them in terms of metals/toxic compounds for protection of public health.

Metals associated with the finer fraction of particulates mostly originate from incomplete combustion of carbon containing materials in motor vehicle, power plants, smelters etc. A study conducted on 12 heavy metals present in air at traffic junctions in Mumbai, India and they found that almost 50–60% of particulates in air could be attributed to vehicular emissions from diesel engines [6]. In urban areas of developing countries, usage of diesel engines has increased several folds in last few decades. Emission inventory data of Delhi [7] suggest that emission contribution from vehicles can be up to 70%. Therefore, there is a need to get an insight into emissions from transport diesel engines operating under different loading conditions.

Diesel engines emit gaseous pollutants and carbonaceous particulates, typically described as diesel particulate matter. Particulate consists of an elemental carbon core with several organic compounds, sulfates, nitrogen-oxides, metals, and irritants (such as acrolein, ammonia, acids, fuel vapors, unburnt lubricating oils) adsorbed to its surface. The particle size distribution and chemical composition of particulates can vary greatly depending on the engine type, engine speed and load, composition of fuel and lubricating oil, and emission control technology [8]. A study of environmental protection agency (EPA) concluded that it is not yet clear if the risk of diesel emissions has decreased over time with improvements in engine technology [9].

Diesel particulate can be characterized in terms of specific metals, elemental carbon, and organic compounds. However, it is not practically possible to speciate all organic hydrocarbons, which may number in thousands. A composite indicator of organic compounds is benzene soluble fraction (BSOF), which represents toxic organic compounds. A study by USEPA concluded that the organic fraction containing neutral and aromatic fraction of diesel soot is mutagenic and carcinogenic in nature [10]. Crebelli et al. established mutagenecity of BSOF of diesel particulates. BSOF has been widely used for assessing the organic fraction, which is mostly toxic [11].

Scientists are constantly working on alternative fuels, which are clean and efficient in combustion. These fuels include compressed natural gas (CNG), biodiesel, alcohols, gas-to-liquid fuels (GTL), dimethyl-ether (DME) etc. For example, CNG has been extensively used as a clean fuel in Delhi and several other cities of the world. There is a need to study possible usage of other alternative fuels at large scale and their impact on human health and environment. It is not feasible to replace diesel engines with CNG engines in cities all over the world. Other alternative fuels need to be examined for engine performance and emission characteristics, followed by environmental and health impact.

Biodiesel is one such fuel which is a carbon-neutral fuel from bio-origin. B20 is a blend of 20% biodiesel and 80% mineral diesel, which may partially replace mineral diesel and can be implemented without significant changes in the existing engine hardware. Biodiesel has also shown potential to reduce the problem of CO_2 emissions and can partly meet energy needs especially in rural areas [12]. It needs to be recognized that biodiesel does

provide an effective alternative to diesel, but unless it is ensured that emissions from biodiesel (especially toxic pollutants) will be lower, or same as diesel, acceptability of biodiesel as a fuel on a large scale may not be forthcoming. Furthermore, there is an immediate need to understand how biodiesel will impact emission control devices and the advanced combustion techniques that the new engines are employing.

In this paper, the main attention is focused on analyzing particulates coming out of engine exhaust from mineral diesel, and biodiesel for the following parameters: Benzene soluble organic fraction (BSOF), trace metals, elemental and organic carbon, engine exhaust particulate surface morphology, size and number distribution.

2. Literature review

2.1. Composition of particulates

Diesel exhaust is a complex mixture of organic and inorganic compounds and gas, liquid, and solid phase materials. Diesel particulates consist of an elemental carbon core with several organic compounds (soluble and insoluble in organic solvents), sulfates, nitrogen oxides, heavy metals, trace elements and irritants (such as acrolein, ammonia, acids, fuel vapors, unburned lubricating oils, moisture) adsorbed to its surface. The organic or hydrocarbon compounds are made up of a continuous gradation of carbon-containing compounds that change from a hydrogen to carbon ratio of 2:1 to eventually a ratio of 0:1 [13]. They include various classes of compounds such as aldehydes, alkanes and alkenes, (both straight and branched chain), and aromatic compounds (single rings, substituted, and poly-nuclear). Any of these species may also contain functional groups such as carbonyl (C=O), hydroxyl (OH) and nitro (NO_2). These organic compounds originate primarily from the unburned fuel and the lubricating oil, although some may be formed during the combustion process and/or reaction with catalysts. The inorganic species include sulfur, oxygen, carbon, and nitrogen-containing compounds such as sulphate (SO_4), carbon monoxide (CO), elemental carbon, and oxides of nitrogen (NO_x). Some of these compounds may also have their origin from the fuel, especially those containing sulfur and carbon [13].

About 90% of diesel particulates encompass a size range from 7.5 nm to 1.0 μm [14] and are therefore important in terms of potential health impacts due to the ability of tiny particles to be inhaled and eventually get trapped in the bronchial passages and alveoli of the lungs. The carcinogenic effects related to diesel exhaust particles is now considered to have at least two components, one related to the inorganic "carbon core" or SOL (solid or insoluble) portion and the other due to the adsorbed organics or SOF (soluble organic fraction) portion.

Most of the particulates emitted by engines lie in the nanoparticulate range (<50 nm), while most of the particulate mass lies in the accumulation mode range that is $50\,nm < D < 1000\,nm$ range [15]. Particle size influences the environmental impact of engine exhaust particles in several ways: it influences the atmospheric residence time of the particles, the optical properties of the particles, the particle surface area and their ability to participate in atmospheric chemistry, and finally, the health effects of the particulates.

The lightest organic compounds remain predominantly in the gas phase; the intermediate ones get partitioned between the gas phase and particulate phase; and the heaviest ones reside predominantly in the particulate phase. Carbonic portion of particulate is the combination of soot and other liquid- or solid-phase materials that are collected, when product (exhaust) gases pass through a filter media. Total carbon present in particulates is often separated into a soluble organic fraction (SOF) and an insoluble solid fraction (SOL).

Organic or soluble fraction present in particulates mainly consist of aldehydes, alkanes, alkenes, aliphatic hydrocarbons, PAH's and PAH derivatives. The organic fraction present in the particulate comes from unburned hydrocarbon, lubricating oil and partially oxidized fuel and oil [16]. The fraction of particulate, which is soot, is often estimated by finding the insoluble portion of the particulate. The fraction of soot in particulate from diesel exhaust varies, but is typically higher than 50%. Soluble organic fraction constituents include unburnt/partially burned fuel/lubricating oil.

2.1.1. Soluble organic fraction

Soluble part of carbonic fraction (SOF) present in particulates dissolve into organic solvents like benzene, and dichloromethane [17]. Here carbonic term has been used in place of organic to avoid confusion as in several texts; term organic fraction is used to represent the part of particulates which is soluble in organic solvents. The soluble organic fraction forms from fuel in two ways: direct and indirect. The direct path is when fuel escapes combustion and simply passes as unburned fuel through the engine. This might happen if some fuel is over-mixed with air, such that there are lean regions of charge or there is too much fuel present in the mixture to support the combustion. The indirect path is when pyrolytic reactions are for some reason interrupted in the conversion of fuel to soot, i.e., if flames are quenched by continued mixing. In such cases, soluble organic fraction will contain pyrolyzed species not originally present in the fuel.

Main source of HC in engines is incomplete combustion due to bulk quenching of flames in a fraction of the engine cycles where combustion is especially slower. Composition of organic fraction can be divided into two distinct sub-groups: compounds that are already present in the fuel and compound that are synthesized from native compounds. The emission mechanism for native organic compounds is comparatively straight forward. The emission mechanism for synthesized organic compounds links to the mechanism of formation of soot. In soot formation, fuel molecules are first cracked or pyrolysed into simpler and smaller molecules and then these simpler molecules build into new structures of ever higher molecular mass which act as soot precursor.

The first step is irrefutable, since light hydrocarbons e.g. methane appear in exhaust gas even when wholly absent from the fuel [18] and hence hydrocarbon emission is composed of native and new born compounds [19]. In the second step, soot formation is interrupted such as by insufficient temperatures or flame quenching or too high or too lean fuel zones, soot precursors are then emitted instead of organic particulates. For instance, polyaromatic-hydrocarbons (PAH's) that are already present in the fuel and which are of molecular mass 128–206 amu (atomic mass unit) are completely distinguishable from the PAH's that are synthesized during the soot precursor formation mechanism, which are of mass (228–350 amu), [20]. This understanding is soundly supported by models [21]. For these reasons, hydrocarbons, organic particulates and carbonaceous particulates are all interlinked by a web of chemical reactions that take place inside the combustion chamber. A conceptual scheme [22] links hydrocarbons in the form of light molecular weight hydrocarbons in the emission (gaseous phase) as organic particulates collected on the filter paper and carbonaceous particulate emission i.e. soot. The organic fraction consists of particulate hydrogen and carbon contained in aliphatics (for example alkanes) and aromatics (i.e. PAH's), and other organically bound elements. A common view of the organic fraction is that it consists of five elements C, H, N, O, S [23] e.g. oxygen as hydroxyl (R-OH), and sulphonates (SO_3–). Some organo-sulfur compounds are also formed in the combustion process, rather than just being unburned fuel remnants [24].

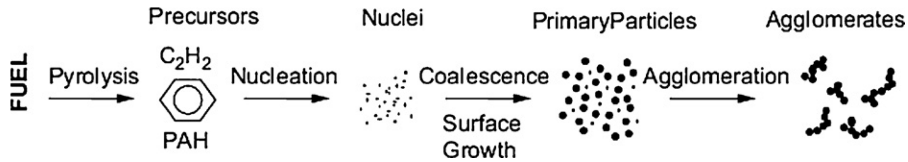


Fig. 1. Schematic diagram of the steps in the soot formation process from gas phase to solid agglomerated particles [23].

2.1.2. Carbonaceous fraction or soot

The SOL or soot is important because it represents the basic solid particles that originate from the combustion process. The other hydrocarbon emissions that is important to characterize is the vapor phase hydrocarbons that are not bound to the particles. This component can be measured by collection of hydrocarbons on an adsorbent, which remain after passing the exhaust through the filter used to remove the particulates.

The evolution of liquid- or vapor-phase hydrocarbons to solid soot particles and possibly back to gas-phase products involve six commonly identified processes: pyrolysis, nucleation, coalescence, surface growth, agglomeration, and oxidation. A sequence depicting the first five of these processes comprise the soot formation process as pictured schematically in Fig. 1, while oxidation, the sixth process, converts hydrocarbons to CO, CO_2 and H_2O at any point in the process. The processes pictured may proceed in a spatially and temporally separated sequence as occurring in a laminar diffusion flame or all of the processes may occur simultaneously as in a well-stirred reactor. In practical combustion systems, the sequence of processes may vary between these two extremes.

Oxidation is the conversion of carbon or hydrocarbons to combustion products. Once carbon has been partially oxidized to CO, this carbon will no longer evolve into a soot particle even after entering a fuel-rich zone. Oxidation can take place at any time during the soot formation process from pyrolysis through agglomeration. The most active oxidation species depends on the process and state of the mixture at that time.

Glassman [25] stated that soot particle oxidation occurs when the temperature is higher than 1300 K. Smith [26] added that soot's graphite-like structure is thought to be responsible for its unusually high resistance to oxidation. Oxidation of small particles is considered a two stage process. First, chemical attachment of oxygen to the surface (absorption), and second, desorption of the oxygen with the attached fuel component from the surface as a product [25]. Bartok and Sarofim [27] suggested that OH most likely dominates soot oxidation under fuel-rich and stoichiometric conditions while under lean conditions, soot is oxidized by both OH and O_2. Haynes and Wagner [28] stated that about 10–20% of all OH collisions with soot are effective in gasifying carbon atoms.

Pyrolysis is the process of organic compounds, such as fuels, altering their molecular structure in the presence of high temperature without significant oxidation even though oxygen may be present. Pyrolysis reactions are generally endothermic resulting in the fact that their rates are often highly temperature dependent [26]. Fuel pyrolysis rates are also a function of concentration. Fuel pyrolysis results in the production of some species which are precursors or building blocks for soot. Soot precursor formation is a competition between the rate of pure fuel pyrolysis and the rate of fuel and precursor oxidation by the hydroxyl radical (OH). Both pyrolysis and oxidation rates increase with temperature, but the oxidation rate increases faster. This explains why premixed flames (where some amount of oxygen is present) are soot less and diffusion flames (no oxygen is present in the pyrolysis region) soot more as the temperature increases. Radical diffusion is important in diffusion flames, especially H, which accelerates pyrolysis when diffused into the fuel-rich zone [25]. Some researchers have suggested that small amounts of O, O_2 and OH radicals might accelerate pyrolysis since many of the reactions take place by means of a free radical mechanism [26]. All fuels undergo pyrolysis and produce essentially the same species: unsaturated hydrocarbons, polyacetylenes, polycyclic aromatic hydrocarbons (PAH's) and especially acetylene. Smith [26] added that if enough O and OH radicals are present, some acetylene is oxidized to relatively inert products. Haynes and Wagner [28] list C_2H_2, C_2H_4, CH_4, C_3H_6 and benzene as typical pyrolysis products in laminar diffusion flames. They also suggested that a decreased residence time in the pyrolysis zone reduces soot formation in diffusion flames. Radicals are also formed during pyrolysis and Glassman [25] suggested that larger molecules increase the radical pool size.

Nucleation or soot particle inception is the formation of particles from gas-phase reactants. Bartok and Sarofim [27] suggested that the smallest identifiable solid particles in luminous flames have diameters in the range 1.5–2 nm, generally referred to as nuclei. The particle inception process probably consists of radical additions of small, probably aliphatic, hydrocarbons to larger aromatic molecules. Particle inception temperatures vary from 1300 to 1600 K. These particle nuclei do not contribute significantly to the total soot mass, but do have a significant influence on the mass added later, because they provide sites for surface growth. Spatially, nucleation is restricted to a region near the primary reaction zone where the temperatures and ion concentrations are the highest in both premixed and diffusion flames [27]. The processes of growth to even larger aromatic ring structures leading to soot nucleation and growth are similar for all fuels and faster than the formation of the initial rings. Thus, the relatively slow formation of the initial aromatic rings control the incipient soot formation rate, which determines the amount of soot formed. Two propynyl radicals, C_3H_3, are likely to form the first ring. The aromatic ring is thought to add alkyl groups, turning into a PAH structure, which grows in the presence of acetylene and other vapor-phase soot precursors. At some point, the PAH is large enough to develop into a particle nuclei, which at this point contains large amount of hydrogen. Haynes and Wagner [28] noted that ring-rupture slows down the rate of soot formation and reduces the final yield. Bryce et al. [29] mentioned three soot nucleation routes. (1) Cyclization of chain molecules into ring structures. An example of this is acetylene molecules combining to form a benzene ring. (2) A direct path where aromatic rings dehydrogenate at low temperature and form polycyclics, and (3) breakup and recyclization of rings at higher temperatures.

Few researchers have also probed into the dependence of the soot oxidation rate upon the length and curvature of the intermediate graphene segments (nanostructures) formed during combustion. Different ratios of edge to basal plane sites or amounts of ring strain imposed by curvature, burnout rates were found to differ by greater than 400% for the soot studied. Surprisingly, the different soot nanostructures were readily produced by using different fuels and pyrolysis conditions. They illustrated this variation between disordered soot derived from benzene and graphitic soot derived from acetylene. Their oxidation rates differ by nearly five-fold. A temperature of 1650 °C was used for acetylene and ethanol pyrolysis while 1250 °C was used for benzene pyrolysis [30,31].

Surface growth is the process of adding mass to the surface of a nucleated soot particle. There is no clear distinction between the

end of nucleation and the beginning of surface growth and in reality the two processes are concurrent. During surface growth, the hot reactive surface of the soot particles readily accepts gas-phase hydrocarbons, which appear to be mostly acetylenes. This leads to an increase in soot mass, while the number of particles remains constant. Surface growth continues as the particles move away from the primary reaction zone into cooler and less reactive regions, even where hydrocarbon concentrations are below the soot inception limit [28]. The majority of the soot mass is added during surface growth and thus, the residence time of the surface growth process has a large influence on the total soot mass or soot volume fraction. Surface growth rates are higher for small particles than for larger particles because small particles have more reactive radical sites [27].

Coalescence and agglomeration are both processes by which particles combine. Agglomeration occurs when individual or primary particles stick together to form large groups of primary particles. The primary particles maintain their shape. Typically, the combined soot particles form chain-like structures, but in some cases clustering of particles has been observed. Exhaust soot from diesel engines consist of primary particles which are spherical in shape which agglomerate to form long chain-like structures. Primary soot particle size appears to vary depending on operating condition, injector type, and injector conditions but most primary particles sizes reported range from 20 to 70 nm. Lee et al. [32] and Bruce et al. [33] used a sampling probe and optical scattering technique, respectively and report primary particles from 20 to 50 nm with an average diameter of about 30 nm. Bruce et al. [33] reported a range of 30–70 nm for the primary particle diameter. In-cylinder light-scattering measurements in diesel engines have produced estimates of 30–50 nm [34] and 40–65 nm [35]. After combustion ends, particles agglomerate further and are seen to be chain-like and typically range in sizes from 100 nm to 2 μm [36] but may become larger. The sampling technique, engine operating condition, injector hardware, and method for determining particle size can have an influence on the reported particle size.

Using the basic measurements, the SOL (sometimes referred to as non-soluble or soot) can be calculated using the following formula:

$$\mathrm{SOL} = \mathrm{TPM} - \mathrm{SOF} - \mathrm{SO_4}$$

2.1.3. Ash fraction/trace metals

Metallic elements emitted by a four stroke heavy duty engine include silicon, copper, calcium, zinc and phosphorous, whereas in two stroke engines, the metallic elements in emissions are lead, manganese, chromium, zinc and calcium [37]. Calcium, phosphorous and zinc are normally present in engine lubricating oil as additives. In some studies zinc, iron, calcium, phosphorous, barium and lanthanum are reported as abundant metals in exhaust [38]. The total emission of metals measured in that study was less than 0.3% of TPM mass, with an emission rate of 1.65 mg/km.

Calcium was found dominant metallic element in diesel particulates, with levels ranging from 0.01% to 0.29% (w/w). Phosphorous, silica and zinc were the next most abundant metallic elements found and sodium, iron, nickel, barium, chromium and copper were barely present and were below detection limits of the instrument [39]. Silicon, iron, zinc, calcium and phosphorous were observed and together constituted up to about 0.5% of total diesel particulates with emission rate of 1.02 mg/km reported as engine transient test emissions of metals for a medium duty truck [40]. From the studies mentioned, it can be inferred that the major elements emitted from diesel engines are Ca, Mg, Zn, Pb, Cr, and Ni. Depending on the origin of fuel, mineral oil metal content in the fuel varies. However, it is also noticeable that the metal contents in lubricating oil also plays an important role in the emission of metal contents in engine exhaust particularly for Ca and Zn.

2.2. Particle size and number distribution

Diesel engines have gone through several phases of development regarding their exhaust emissions. EPA imposed norms in 1997 on mass of total particulate matter (TPM) forced engine manufacturers to again go through series of changes in fuel injection systems and compression ratios. These changes certainly lowered down the TPM mass or number of bigger particles caused by unburnt or partially burnt fuel. But further research has shown that it is not the mass which was most threatening but the number of particles. Numberwise, more than 90% of the TPM are fine particles range from 5 to 50 nm, whereas these particles represent less than 10% mass of the TPM. These fine particles can be inhaled and eventually trapped in bronchial passages and alveoli of lungs. Hence, reduction in mass of TPM never ensures reducing the number of fine particles. On the other hand, there is always a possibility of increased number of such particles which has been reported in some studies by use of very high pressure injection systems that are being fitted in every diesel vehicle now-a-days.

If one is solely interested in mass concentration, then accuracies in measuring the nucleation mode will not appreciably alter the result. On the other hand, if one just wishes to investigate the number concentration, then inaccuracies in measuring the accumulation mode would be of lesser value. Diffusion governs particle transport particularly strongly in the nucleation mode and hence potentially affects the number distribution; whereas inertial deposition has greater implications for the accumulation mode [15].

Nucleation mode particles are more vulnerable to measurement falsification than accumulation mode particles. Sole reason for such falsified results can be laid on the volatile component and highly non-linear nature of nucleation. Nucleation mode particles are created or destroyed according to how the exhaust is diluted, whereas accumulation mode particles consist of a solid carbonaceous core and are only affected by saturation and peak temperatures.

It is possible to lay down a clear principle when attempting to control the particulate emissions from a motor vehicle. The dominant factor here is the proportion of volatile (sulfates and organics) to non-volatile (carbonaceous and ash) particulate. If latter is strongly present, it will scavenge the volatile material; this will keep down the saturation and hence nucleation will be suppressed. On the other hand, if volatile material will be in excess, then insufficient solid area for adsorption and condensation will promote nucleation. For example, high engine load favors carbonaceous particulate formation and low engine load favors organic particulate formation.

2.3. Health effects of diesel particulates

Diesel particulates have a very large surface area, which makes them an excellent carrier for adsorbed inorganic and organic compounds. Ultra fine particles emitted from diesel engines are very high in number, invariably more than millions of particles per cubic centimeter, but they contribute little to the total particulate mass. The highest deposition efficiency in the alveolar region of the lungs is shown by particles having a diameter of ~20 nm. Ultra fine particles can not only penetrate the epithelium but also enter into the blood stream. In fact, these particles have been detected in the interstitium of the lung as well as in the blood streams shortly after the exposure [41].

Exposure to the diesel exhaust may cause acute and chronic non-cancer respiratory effects and has the potential to cause lung cancer in humans. As diagnostic tests are unable to prove causality, epidemiologic studies are utilized for decoding the relationship

between natural variability in exposure and variability in rates of illness [42]. The diesel engine exhaust and related toxicity has been evaluated in numerous acute and chronic studies. Laboratory animals especially mice and canines are considered as good models for humans with regard to their responses to DPM [43,44]. Depending upon rural or urban location, the annual mean exposure to diesel exhaust is estimated to be about 1 to 4 $\mu g/m^3$ of inhaled air [45]. There are numerous studies that have shown that diesel exhaust exposure can cause acute eye and bronchial irritation, nausea, lightheadedness, phlegm and cough. More than a dozen chronic studies involving laboratory rats, mice, hamsters, guinea pigs, cats and monkeys have studied the respiratory and systemic effects due to exposure to DPM [44,46]. Acute exposures to high concentrations of fresh diesel exhaust can cause respiratory inflammation and symptoms. Nasal deposition of large doses of diesel exhaust amplifies immunological response to antigens. Lifetime exposures of rodents to high concentrations cause chronic inflammation and fibrosis. The semi volatile and soot-borne organic material is mutagenic; soot extract is carcinogenic to mouse skin, and inhalation exposures of rats to high concentrations cause lung tumors.

Several recent laboratory studies with rats have indicated that the SOF portion of DPM is an important precursor for tumor formation [47–50]. The associated SOF, particularly the PAH and the nitro-PAH could have a significant contribution to the overall carcinogenic effect. Exposure to diesel exhaust in presence of other air pollutants can be even more harmful (for example, increased susceptibility to certain allergies, increased toxicity of diesel particulates in the presence of ozone and NO_x). There is no diesel exhaust specific information that provides direct insight to the question of variable susceptibility within the general human population and vulnerable subgroups, including children and elderly and subjects with pre-existing respiratory illness. However, further research is needed to improve the knowledge and database on exposure to diesel exhaust and potential human health effects, and thereby reducing uncertainties of future risk assessments. Researchers have carried out tests using animal models to determine the mechanisms associated with pulmonary cancer caused by diesel exhaust particles [51]. One such study indicated that the deposition of metals (like iron) on the lower airway would generate hydroxyl radicals which would trigger the production of free radicals and finally cause both acute and chronic lung injuries [52].

The chemical form and oxidation state of metals affect their toxicity. Advanced techniques are desired for speciation of toxic metals. Few recent findings have indicated that these metals activate epidermal growth factor receptor (EGFR) and lead to increase in the levels of guanosine triphosphate-bound Ras in human lung cells [53]. Iron, along with other transition metals such as Cu and Zn have well-documented ability to generate free radicals via Fenton chemistry. Transition metals and iron in particular, can be present in high levels in DPM [54]. The transition metals must undergo redox-cycle to be capable of generating hydroxyl radicals, which cause the major injury to macromolecules and this is accomplished via reductants commonly found in the lungs e.g. superoxide anion glutathione, ascorbate [55]. Transition metals are responsible for activating pro-inflammatory transcription factors such as NF-kB in epithelial cells hence directly linking transition metal content to inflammation [56].

Several studies have shown that lifetime exposures to very high concentrations of diesel particulates result in the development of lung tumors among the animals. Overload of diesel particulates and consequent persistent inflammation and cell proliferation is suggested as plausible mechanism by which tumors develop, indicating a nonlinear mode of action for lung cancer in the rat [43,46]. The response for some of these studies has been recorded at relatively high exposures to diesel exhaust (>3500 $\mu g/m^3$ of diesel particulates).

Diesel particulate undergoes numerous atmospheric reactions, including photolysis, nitration, and oxidation. The atmospheric chemistry of organic compounds associated with diesel particulate is fairly complex. Researchers [57] have studied the effect of ageing and solar radiation on diesel exhaust by simulating such artificial environments within chamber. Recently, it has been reported that treatment of diesel exhaust particulates with ozone increased the inflammatory potential in rat lungs [58]. There is also some evidence for possible immunologic effects and exacerbation of allergenic response to known allergens. Recent experimental studies highlight the role of diesel particulates in enhancing inflammatory and allergic responses in the respiratory system [59–63]. It has been observed with animal studies that gaseous co-pollutants like ozone, NO_x and SO_2 significantly enhance the pulmonary inflammatory potential of ultra fine carbonaceous particles. The role of surface chemistry has been emphasized in the overall toxicity due to ultra fine particles. Aged and experimentally sensitized rats have shown higher sensitivity to higher dosage of ultra fine carbonaceous particles. The ultra fine particles in these cases were not effectively phagocytized by the alveolar macrophages upon their deposition in the deeper parts of the lungs [41,64]. Furthermore, translocation of ultra fine particles to the liver and even to neurons has been documented [65].

Studies on the health effects of diesel exhaust have until recently focused primarily on cancer outcomes [66]. However, in recent years, attention has begun to focus on understanding the non-cancer respiratory effects of diesel exhaust and their possible role in the acute or chronic health effects of airborne PM. There is emerging experimental evidence of irritants and/or immunologic effects of diesel exhaust on the respiratory system. In addition, recent epidemiological studies have demonstrated association between residential proximity to traffic sources and adverse respiratory outcomes, including asthma hospitalization among children, increased respiratory symptoms, and diminished lung function [41,67,68]. Exposure assessment in these studies has included self-reported traffic volumes on residential streets (e.g., high, medium, or low), quantitative data on traffic volumes collected by local agencies, and, occasionally, air monitoring data at selected locations. Because of the limitations of the exposure data, it is not always possible to uniquely implicate diesel exhaust as distinct from other forms of motor vehicle exhaust in the observed respiratory health effects. These findings show novel mechanisms of action by metals and may provide insight relevant to the health effects of diesel particulate exposure.

2.4. Biodiesel: An oxygenated fuel

Alternative diesel fuels or oxygenates are simple organic compounds, the functional groups of which contain oxygen in some form for example alcohol (R-OH), esters (RCOO). One of the important oxygenated fuel is biodiesel; which contains esters derived from the process of transesterification [69] (Fig. 2) of vegetable oils e.g. Cotton seed, Rapeseed, Soybean, Peanut, Karanja and Jatropha etc.

Oxygenates are burned neat or more typically as oxygenate-diesel blends and their particulate suppressing properties are well documented. Oxygenated additives are known to reduce soot formation in diesel engines [70]. Before choosing any particular oxygenate as a renewable fuel for technical feasibility, a wide range of criteria other than reliable clean burning combustion must be checked. Examples of that criteria can be ignitability, long term stability, corrosivity, polymerization compatibility, toxicity, lubricity [71], solubility in diesel [72], viscosity, volatility [73] and degradability. There is also susceptibility to injector nozzle coking [74], especially in case of straight vegetable oils utilization.

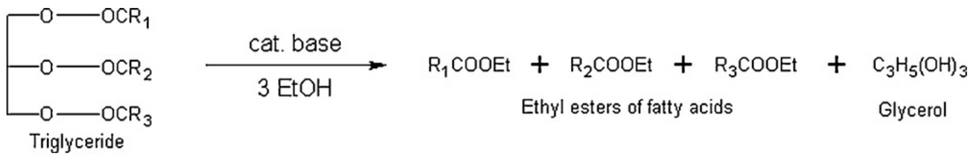


Fig. 2. Process of transesterification for conversion of vegetable oils into biodiesel.

In their particulate suppressing action, oxygenates are as potent as organo-metallic fuel additives, but with two important differences: (i) there is no incombustible ash, and (ii) blends are at percentage rather than ppm levels. Because of this second difference, oxygenates are more aptly designated as fuel components rather than fuel additives. One can expect some modifications in energy release rates also, due to calorific value differences. If bulk fuel properties such as density and viscosity are altered, then certain effects might be observed not in the combustion, but in the geometry of fuel spray, the atomization of the fuel or even in the flow characteristics of fuel within the injector nozzle. Certain fuels like B100 would be called as an alternate fuel but they are used in practice only to a limited extent because of the uneconomical prices however there is a logic in carrying out experiments on B100. Since the engine behaves very well with B100 and B0 (mineral diesel), it is expected that the engine will behave normally to any blend of biodiesel and diesel. Using B100, accelerated tests can be performed. Moreover, biodiesel and diesel have almost same physical fuel properties but they are not the same fuel. The particulate fraction targeted with oxygenates is soot. The absence of incombustible ash in oxygenates makes them a no-participant responsible for metal emissions. Since oxygenates denote purely organic compounds, it leads to no contribution towards ash fraction and also their sulfur levels are low or negligible, which results in no contribution to the sulphate fraction. These are some welcome facts which make oxygenates a desired partial replacement for mineral diesel.

A recent study examined factors impacting the stability of Biodiesel (B100) samples collected as part of a 2004 nationwide fuel quality survey in the United States. The survey included samples produced from soya, waste oils, and tallow. Test for insoluble fraction formation and the oxidation stability method (via Rancimat apparatus) for induction time were carried out. Additionally, the samples were characterized for fatty acid make up, relative antioxidant content, metal, and total glycerin content (free glycerin plus glycerin bound as mono-, di-, and triglycerides). In the oxidation stability test, the sample was exposed to air at 110 °C. The stream of air carried volatile carboxylic acids (primarily formic acid) formed in the oxidation reaction into an absorber that contains demineralized water [75]. The amount of acid was quantified by measuring the increase in conductivity of the water over time. For the samples examined, the polyunsaturated content (or oxidizability) had the largest impact on both increasing insoluble fraction formation and reducing induction time (which was the time from the beginning of the air purge until a sharp increase in the conductivity was observed) [76].

Variable effects are observed on the organic fraction e.g. the particulate mass is lower but the carbonaceous organic ratio remains unchanged, suggesting that both the fractions are proportionally decreased [77]; or there is no consistent trend [78]. More commonly filter deposits are ‘wetter’ and lighter in colors [79]; both observation suggests greater organic fraction [80] i.e. preferential reduction in soot [81] or perhaps of greater gas to particle conversion among organic compounds than with diesel. Filter deposits may also become lighter simply because the reduction in carbonaceous particulate allows lubricant derived organic particulate to become more prominent by proportion [81] or increase in organic particulate out-weights the decrease in carbonaceous particulate [82]. Smoke readings responding to blackness register only decrease in carbonaceous particulates [83]. This improvement is largely cosmetic if organic compounds are emitted in greater quantities, which is a note of caution before biodiesel go on a full scale production. Contrary trends between hydrocarbon and organic particulates [84] suggest subtle differences in gas to particle conversion and in volatilities between oxygenates and diesel fuel e.g. with biodiesel, the organic fraction has a larger contingent of high molecular weight compounds than with diesel [85]. Exhaust gas analysers are designed to analyze conventional diesel fuel hence factious conclusions may arise through blind adherence to the same protocols with oxygenated fuels.

A study conducted on eight oxygenates showed that ether demonstrated greatest particulate reduction potential [86]. Another study on fourteen oxygenates showed alcohol as having greatest particulate reduction potential [77]. Some studies showed a inversely proportional relationship between the mass of soot in the particulate and the mass of oxygen in the fuel [86]. Comparison of fuels by their oxygen content, rather than oxygenate content seems more appropriate though it will be a bit more complicated than just volumetric ratios. Fuels containing ∼30–40% oxygen have been reported to produce very good results [87]. This proportionality supplies the most obvious clue as to how oxygenates reduce soot. The soot suppression seems not to arise simply through displacing diesel fuel; and it might equally proceed through discouraging soot formation or encouraging soot oxidation as both routes accomplish the same aim. Another argument can be about the combustion process itself particularly because fuel rich regions are having additional oxygen from fuel therefore oxidation reactions take place in preference to pyrolytic reactions [88]. Effectively, this means that the combustible mixture is supplied with additional oxygen (via the fuel), contrary to external oxygen (via the air) which has no part in excess oxygen. In fact, the same justification is used for supplying ethanol-gasoline blends as high speed fuels to provide the combustible mixture with more fuel borne oxygen and thereby to restrict emissions of CO.

3. Experimental setup

3.1. Engine setup

For the comparative study of biodiesel and mineral diesel, a direct injection, medium duty transportation engine (Mahindra, India, MDI-3000) was used. Detailed specifications of this engine are given in Table 1. The engine was coupled with an eddy-current dynamometer (Schenck Avery India, ASE70). The eddy current dynamometer was equipped with a suitable dynamometer

Table 1
Mahindra DI engine specifications.

Manufacturer	Mahindra & Mahindra Ltd., India
Model	MDI 3000 A
No. of cylinders	Four, in-line
Combustion system	Direct injection
Bore/Stroke (mm)	88.9/101.6
Engine displacement (cc)	2520
Compression ratio	18:1
Rated load	144 N m at 1800 rpm
Rated power	40 hp at 2300 rpm

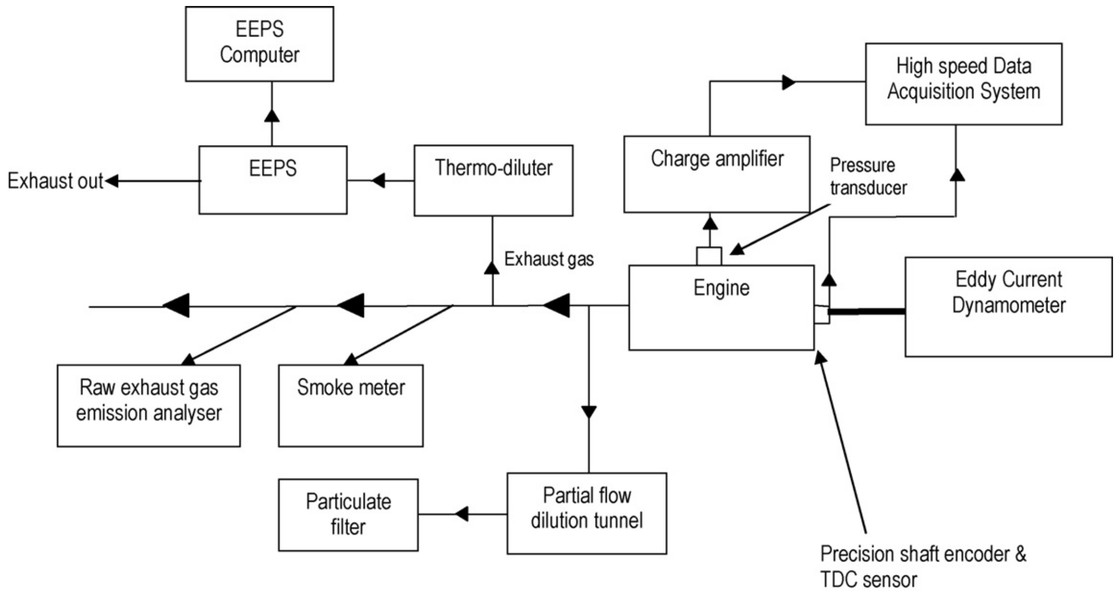


Fig. 3. Schematic diagram of Mahindra DI engine experimental set-up.

Table 2
Dynamometer and controller specifications.

Manufacturer	Shenck-Avery Ltd., India
Model	ASE-70
Operating principle	Eddy current
Maximum Torque	328 N m
Full scale torque	527 N m
Maximum allowable error in measurement	0.25% full scale torque 1.31 N m
Display units	Digital torque indicator Digital rpm indicator 6 channel temperature indicator
Weight	Approx 500 kg
Operating temperature	Up to 45 °C
Maximum rpm	6000

controller, which was capable of absorbing maximum power and torque generated by the engine at every load and speed combination in a very short time. Dynamometer specifications are given in Table 2.

The schematic diagram of the experimental setup is shown in Fig. 3. The engine is installed with an eddy current dynamometer and a dynamometer controller. The engine cylinder head is installed with a peizo-electric pressure transducer and a charge amplifier. A precision shaft encoder and a TDC sensor are also installed in the engine shaft. All these signals are acquired by high speed data acquisition system, where they are processed to yield pressure-crank angle history. The exhaust gas from the engine passes through an exhaust line. Part of the exhaust is drawn into the partial flow dilution tunnel, where particulate sampling is done for metal analysis, BSOF estimation and particulate morphology. Another part of the exhaust with the aid of a pump is diluted in a thermo-diluter. This stream then passes through EEPS where particulate size and number density is measured. Smoke opacimeter and raw exhaust gas emission analyzer are used for measurement of exhaust opacity and exhaust gas composition repectively.

3.2. Particulate measurement system

The Engine Exhaust Particle Sizer (EEPS^{TM}) measures the size distribution of engine-exhaust particulate emissions in the range from 5.6 to 560 nm with the fastest time resolution available.

The EEPS spectrometer displays measurements in 32 channels total (16 channels per decade). It operates over a wide particle concentration range, from 10^8 particles/cm^3 to 200 particles/cm^3. It operates at ambient pressure to prevent evaporation of volatile and semi-volatile species, and it does not require any consumables. The instrument (Fig. 4) used in the lab has a unique rotating disk method to dilute the sample for measurement. Each unit is supplied with two disks: one with eight cavities and the other with ten cavities. This allows one to select a dilution ratio ranging from 15:1 to 3000:1.

Earlier methods of sub-micrometer sizing required stable aerosol and, therefore, do not meet the requirements of engine test benches and chassis dynamometers where dynamic changes in both particle number and size distribution takes place as the engine undergoes different steps of test cycles. The EEPS uses a unique charging system and multiple electrometers to get signals

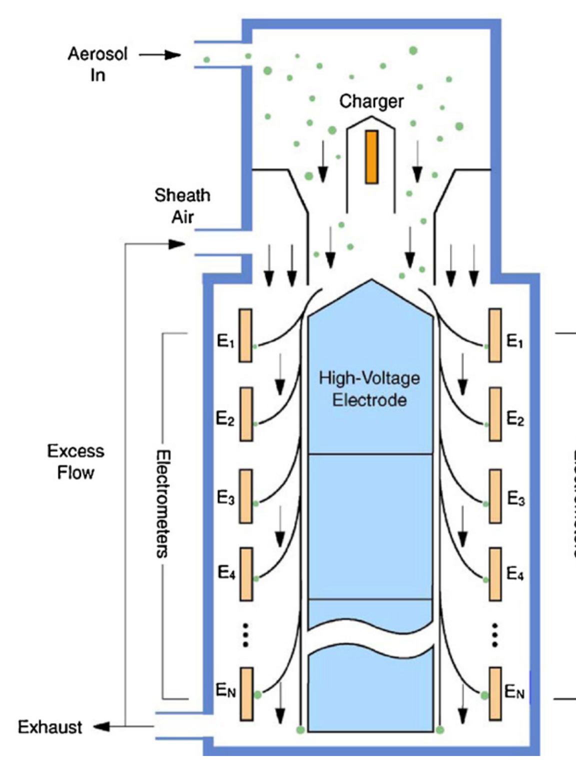


Fig. 4. Schematic diagram of EEPS (Make: TSI Inc., USA).

Table 3
Specifications of engine exhaust particle sizer (model 3090).

Particle size range	5.6–560 nm
Particle size resolution	16 channels per decade (32 total)
Electrometer channels	22
Charger mode of operation	Unipolar diffusion charger
Inlet cyclone 50% cut point	1 μm
Time resolution	10 size distributions per second
Aerosol	10 L/min
Sheath air	40 L/min
Inlet aerosol temperature	10–52 °C
Operating temperature	0–40 °C
Storage temperature	−20–50 °C
Atmospheric pressure correction range	700–1034 mbar
Humidity	0–95% RH (non-condensing)
Data averaging	0.2–60 s
Dimensions (LWH)	70.4 cm × 34.3 cm × 43.9 cm
Front panel display	6.4-inch color VGA LCD
Weight	32 kg
Power requirements	100–240 VAC, 50/60 Hz, 250 W

from all particle sizes simultaneously. The electrometer current data is processed in real time with a high-performance Digital Signal Processing (DSP) chip inside the instrument. This corrects for multiple charges and the time delay between electrometers. The data is then processed further to give results in 32 equally spaced (log-scale) size channels. This data is displayed on the instrument and sent to a computer for long-term storage and display.

The EEPS Model 3090 uses a corona charger to put a predictable charge level on the particles. The charged particles are introduced near the center of a column. An electric field inside the column repels the particles outward, where they are measured using an array of precision electrometers connected to electrodes on the outside wall of the column. This “Inside-out Differential Mobility Analyzer” arrangement allows for concentration measurements of multiple particle sizes simultaneously. The detailed specifications of the equipment are given in Table 3.

3.3. Elemental analysis

Inductively coupled plasma optical emission spectrometry (ICP-OES), is an analytical technique used for the detection of trace metals. It is a type of emission spectroscopy that uses inductively coupled plasma to produce excited atoms and ions that emit electromagnetic radiation at wavelengths characteristic to a particular element. The intensity of this emission is indicative of the concentration of the element within the sample.

Argon gas is used to create the plasma. A peristaltic pump delivers an aqueous or organic sample into a nebulizer where it is atomized and introduced directly inside the plasma flame. The sample immediately collides with the electrons and other charged ions in the plasma and is broken down into charged ions. Various molecules break up into their respective atoms which then lose electrons and recombine repeatedly in the plasma, giving off the characteristic wavelengths of the elements involved which are compared with those emitted by pure standards to derive elemental concentrations in the given sample.

3.4. Experimental test matrix

Tests were performed for the comparison between biodiesel and mineral diesel. These were for:

1. Benzene soluble organic fraction (BSOF)
2. Elemental and organic carbon (EC/OC)
3. Metal traces
4. Engine exhaust particulate morphology (SEM imaging)
5. Number and size distribution of engine exhaust particles (EEPS)

Table 4
Variable load matrix for Mahindra DI engine.

Speed (rpm)	Load (% of max load)
1800	0%
1800	20%
1800	40%
1800	60%
1800	80%
1800	100%

Table 5
Variable speed matrix for Mahindra DI engine.

Load (% of max load)	Speed (rpm)
50%	1400
50%	1700
50%	2000
50%	2200
50%	2400

Sampling procedure for comparative study of biodiesel and mineral diesel comprise of operating the engine at different speeds and loads. Engine was operated on some specific operating points, which have been shown in Tables 4 and 5. Variable speed test was done up to 2400 rpm only because the number of particles in exhaust reached the upper limit of the engine exhaust particle sizer (EEPS). Table 6 shows the sampling duration and choice of filers for sample collection for various analyses such as trace metals, BSOF and particulate morphology using scanning electron microscopy.

3.5. Sampling and analysis details

3.5.1. Filter papers

Particulates emitted from engine tail pipe after dilution through partial dilution tunnel was collected through Tissue-Quartz filter (QF/A, 47 mm, Whatman), as specified in NIOSH method 5040 for elemental carbon (diesel particulates). Filters were kept in desiccators for 12 h before and after sample collection, which ensured precise measurements of mass of particulates.

3.5.2. Quality control and calibration of instruments

Commercially available multi-element standard (Merck) solutions were used for all metals except Na. For Na, standard solution was prepared in the laboratory. Working standard solutions of three different concentrations were prepared by diluting standard solutions either procured from manufacturer with Milli-Q water or by diluting the standard solution made in the laboratory. These standards were stored at 30 °C in inert bottles. The calibration was done by using the blank solution to reset the instruments. The standards were then analyzed with the lowest concentration first and then moving on to higher concentrations. In order to ensure the consistency and also to check the maximum possible extraction of heavy metals from the samples, the following procedure was adopted.

1. All the glassware and filter assembly was subjected to acid wash and dried to avoid any contamination from previous samples.
2. Blank samples were analyzed to check the possible contamination and interference from various reagents and glassware used

Table 6
Sampling duration and choice of filters for various tests.

S. No	For analyzing	Type of filter	Duration of sampling (min)
1	Trace metals	AQ F/A (047) Tissue-quartz	5–7
2	BSOF	AQ F/A (047) Tissue-quartz	30–35
3	SEM	GF/A (047) Glass fiber	30

in the analysis. It was found that the concentration of various metals in the blanks were very low.
3. Glass vessels were thoroughly cleaned with 4% concentrated HNO_3 and Milli-Q water.

3.5.3. Test procedure for heavy metals and BSOF estimation

Initially, filter papers were desiccated for 12 h in anhydrous silica gel desiccator and then weighed. For collecting a sample, one filter paper was placed in filter holder assembly, which was installed in the partial flow dilution tunnel. After running the engine at desired load and speed and collecting the particulates through partial flow dilution tunnel for a predetermined period of time, the filter papers were removed carefully from the filter assembly and again kept in desiccator. These filter papers were then analyzed for characterization of metals and BSOF in particulates.

3.5.4. Extraction of samples for heavy metal analysis in particulates

In the present study, sample extraction was carried out using hot plate digestion method [89]. This digestion procedure is used for preparing samples, which are to be analyzed by ICP-OES (Thermo, USA; 6300 duo ICAP). One half of the particulate laden filter was cut into small pieces using plastic scissor and then put into an inert bottle, in which 15 ml of concentrated HNO_3 (Suprapure, Merck) was added. The remaining half of the filter paper was taken in similar way into another bottle. Temperature of each sample was raised to 175 °C in less than 5.5 min and maintained at 175 °C for more than 4.5 min. After digestion, the acid from the two vessels was combined and filtered through 0.22 μm Millipore filter paper. The filtrate was measured and diluted three times with Milli-Q water and then stored in inert bottles. Reference was taken as analytical blank filter paper and 30 ml of conc. HNO_3 (Suprapure, Merck), 10% of blanks from the same lot of filter papers are used to get a best representative average blank concentration. By the above described method, concentrations of Ca, Cu, Cr, Mg, Fe, Na, Ni, Pb, and Zn were determined.

3.5.5. Estimation of benzene soluble organic fraction (BSOF) in particulates

ASTM test method D 4600-87, ASTM 2001 was used for estimation of BSOF in particulates [90]. Before sampling filters were desiccated for about 12 h. After sample collection, particulate laden filters were kept for desiccation for another 12 h and their final weight was noted. Filters were cut into small pieces using metal scissor and inserted into a reagent beaker; thereafter 20 ml of benzene was added to it. This reagent bottle was kept in ultrasonic bath for 20 min thereafter sample was decanted and filtered through 0.45 μm Millipore filter paper. The filtrate was collected in a 100 ml beaker. The procedure was repeated with another 10 ml of benzene in the same reagent beaker. This 100 ml beaker was covered with aluminum foil having holes and was kept in oven at 40 °C for 12–18 h until the sample dried. The beaker was allowed to cool down to room temperature. The initial and final weight of the beaker was measured to estimate the total mass of benzene soluble organic fraction in the sample. In order to check the reference concentration, blank filters were used for BSOF extraction as per the same ASTM standard.

3.5.6. Estimation of metals in mineral diesel, biodiesel and lubricating oil

The fuels used in this study were (#2) diesel and biodiesel, which meets the ASTM specifications. The sample preparation of mineral diesel, biodiesel, and lubricating oil was carried out using fast response temperature controlled furnace. 0.5 g of any fuel or lubricating oil was taken in an inert vessel to which 9 ml concentrated HNO_3 was added. EPA 3052 method was used for this digestion [91]. Temperature of each sample was raised to 180 °C in 5.5 min and kept at 180 °C for another 9.5 min. After digestion, the acid was measured and was diluted three times with Milli-Q water and stored in inert bottles. This solution was then filtered by 0.22 μm filter. Concentrations of Ca, Cd, Cr, Fe, Mg, Ni, Na, Pb, Zn, and Cu were determined in all above samples using ICP-OES.

Table 7
Concentration of various metals in diesel, biodiesel and lubricating oil samples.

Metals	Diesel (μg/g)	Biodiesel (μg/g)	Lubricating oil (μg/g)
Ca	902.3	721.2	2046.8
Co	2.3	1	2.6
Cr	58.7	62.9	76
Cu	9	2.4	4.3
Fe	402.3	419.8	827
Mg	1162.3	1996.9	3618.1
Ni	31.8	1.2	76
Pb	8	2.8	8
Zn	271	350	832.4

3.5.7. Estimation of elemental and organic carbon

The procedure followed in this study to determine particulate carbon content is similar to the method described by Cachier et al. [92]. A DPM-laden thimble was divided in two parts. The first part was fed into TOC (total organic carbon) analyzer (TOC-5000 (A)/5050 (A) Solid Sample Module, Shimadzu Corporation, Japan) for analysis of total carbon (TC). The second part of the thimble was kept in oven at 340 °C for 100 min to get rid of OC and then the thimble is fed into CHN/O/S elemental analyzer (CE 440, Leeman Labs Inc., USA) to obtain the EC content. The OC value was taken as the difference between TC and EC (assuming inorganic carbon content in sample is negligible). TOC analyzer was calibrated using known quantity of ultra pure glucose and CHN/O/S analyzer was calibrated using standard acetanilide (carbon 71.09%). The entire analysis was repeated twice for every sample. In all analyses (metals, BSOF, OC, and EC), thimble blanks were taken and subjected to identical extraction and analysis procedures and blank corrections were made for all the samples [93].

3.5.8. Scanning electron microscopy for particulate morphology

The samples of particulates were collected on filter papers mounted on partial flow dilution tunnel and the sampling duration was kept constant at 30 min for all the investigations. The soot collected was essentially non-conducting in nature therefore gold sputtering was carried out on all the samples. Thereafter the scanning electron microcopy was carried out for the samples. The magnification for all the micrographs was kept at 1000×.

3.5.9. Size and number distribution of particulates

The size and number distribution of particulates in the exhaust was measured using engine exhaust particle sizer. The experiments were carried out at (i) varying speed at constant engine load and (ii) varying load at constant engine speed. The experiments were carried out for mineral diesel, 20% blend of biodiesel (B20) and biodiesel (B100).

4. Results and discussion

The results related to mineral diesel, lubricating oil, and biodiesel metal composition are used in this paper extensively and are given in Table 7.

Data given in Table 7 represents X μg of any specified metal present in the 1 g of the fuel/oil. The blank tissue papers were analyzed for the metals present in them (Table 8) and this data is used for blank filter paper correction. Table 8 presents the background

Table 8
Average metal presence in blank (tissue-quartz) filter samples.

Metals	Concentration (μg/g)
Ca	793.8
Cr	27.7
Cu	12.3
Fe	103.5
Mg	498.1
Na	861.0
Ni	2.7
Pb	12.0
Zn	162.7

levels of different metals present in the filter matrix. It does not correspond to any particular fuel as such but these background levels are subtracted from the results obtained for the respective PM emitted from engine using different types of fuels (diesel and biodiesel).

10% (Nos.) analytical blank filters were used for determining metal concentrations in blank filters using ICP spectrophotometer. Overall five filters were analysed were blank correction, and Table 8 represents average concentration of metal present in these blank filters. Concentration was represented in terms of weight of metal present in blank filter per gram of filter weight.

All the data presented in this paper has been corrected for the average blank readings. Typical weight of a tissue-quartz filter lies between 0.14 and 0.15 gm, so contribution of blanks in exhaust particulate samples was miniscule.

4.1. Metals in particulates from B100, B20 and mineral diesel fuelled engine

Experimental study with biodiesel showed that there are some metals, which are found in excess in diesel exhaust whereas there are some other metals which are found in excess in biodiesel exhaust.

Experimental study was done to characterize the effect of engine operating conditions (speed and load variation) on particulate emissions. The discussion would be divided into two parts; metal concentration in particulate with (i) varying load condition at constant speed and with (ii) varying speed conditions at constant load.

4.1.1. Metal concentration in particulates with variation of engine load at constant speed

An experimental study was carried out to study the effects of load variation on concentration of metals in particulates coming out in engine exhaust, at 1800 rpm.

At low engine loads or more specifically at no load, combustion temperatures are relatively lower, which implies that for low combustion efficiency, a large fraction of fuel injected into the combustion chamber goes out in the form of exhaust without complete burning. This is a primary reason for high metal concentrations at low load condition as fuel itself is the principal source for metal presence in exhaust particulates.

Calcium (Ca): As mentioned in the Fig. 5, Ca concentration in mineral diesel is higher than biodiesel, which is reflected in the graph too. At higher engine loads, Ca concentration in diesel supersedes the concentration of B20 or B100 exhaust particulates.

Chromium (Cr): Fig. 5 shows Cr content in particulates drawn from diesel, biodiesel and B20 exhaust at varying engine load conditions. B100 exhaust shows the highest concentration of Cr at low loads but as the load increases, Cr concentration in diesel increases rapidly and exceeds the Cr concentration in B100. Biodiesel contains maximum Cr as a constituent (Diesel 58.7, B100 62.9, Lubricating oil 76 μg/g) however at higher engine load, high Cr is observed in diesel exhaust possibly due to relatively higher wear of chrome plated piston rings.

Copper (Cu): Fig. 5 shows Cu content in particulates drawn from diesel, biodiesel and B20 exhaust at varying engine load conditions. It can be seen from the graph that Cu is below detection limits for B100 exhaust, but present in diesel and B20 exhaust particulate.

Iron (Fe): Fig. 5 shows Fe content in particulates drawn from diesel, biodiesel and B20 exhaust at varying engine load conditions. It can be observed from the graph that B100 showed highest concentration of iron, and the sources of iron in engine exhaust is fuel itself (Table 7). Diesel has 402.3 μg/g, biodiesel has 419.8 μg/g and lubricating oil has 827 μg/g iron in the fuel. Engine wear also contributes to the iron concentration in the particulates.

Magnesium (Mg): Fig. 5 shows Mg content in particulates drawn from diesel, biodiesel and B20 exhaust at varying engine load conditions. It is visible from the graph that B100 shows the highest concentration of Mg. As load increases, Mg concentration for B100 decreases very rapidly and becomes even lower than diesel and B20 particulate.

Sodium (Na): Fig. 5 shows sodium content in particulates drawn from diesel, biodiesel and B20 exhaust at varying engine load conditions. Sodium is found in abundance in biodiesel, diesel and lubricating oil. It can be seen in the Fig. 5 that Na concentrations are very high compared to any other metal. Diesel has shown highest concentration of Na ranging from 45 to 90 mg/g. B100 has shown the lowest Na concentration among all these ranges from 15 to 65 mg/g. B20 exhaust particulate's sodium concentration is in between them and the same trend is also observed in the particulates also.

Nickel (Ni): Fig. 5 shows nickel concentration in particulates drawn from diesel, biodiesel and B20 exhaust at varying engine load conditions. As it is mentioned in the Table 7, diesel has 31.8 μg/g, B100 has 1.2 μg/g and lubricating oil has 76 μg/g Ni concentration. Ni concentration for mineral diesel keeps on increasing with increasing engine load. B100 and B20 both do not show any trace of nickel in their exhaust. Biodiesel's self lubricity properties and smaller concentration of Ni in fuel seem a possible reason for this.

Lead (Pb): Fig. 5 shows lead concentration in particulates drawn from diesel, biodiesel and B20 exhaust at varying engine load conditions. Biodiesel has 2.8 μg/g, mineral diesel has 8 μg/g and lubricating oil has 8 μg/g lead as constituent (Table 7). From the figure, it can be seen that diesel exhaust particulates show the highest lead concentration among all fuels and B100 exhaust particulates show the lowest Pb concentration.

Since biodiesel and lubricating oil both do not have significant lead hence lead coming into biodiesel exhaust can be mainly from engine wear and to a lesser degree, contribution from lubricating oil combustion.

Zinc (Zn): Fig. 5 shows zinc concentration in particulate drawn from diesel, biodiesel and B20 exhaust at varying engine load conditions. B100 particulates show highest Zn concentration for all engine load conditions.

Metals which are found in the fuels decrease as the load increases. Metals which come from lubricating oil increase as the load increases. Metals, which come from the engine wear also increases with the increase in engine load.

For the metals, which are found in biodiesel, lowest values of these metals present in particulates are found at 100% load condition whereas metals which are found in mineral diesel, lowest values of these metals are found at 60–80% load conditions. For mineral diesel at 100% rated load, fuel quantity injected is maximum hence there are several fuel rich zones where combustion does not take place efficiently and unburned fuel come out in the form of engine exhaust particulates. For biodiesel at 100% load, there are relatively lesser fuel rich regions because of the fuel's oxygen content hence its metal concentration keeps on

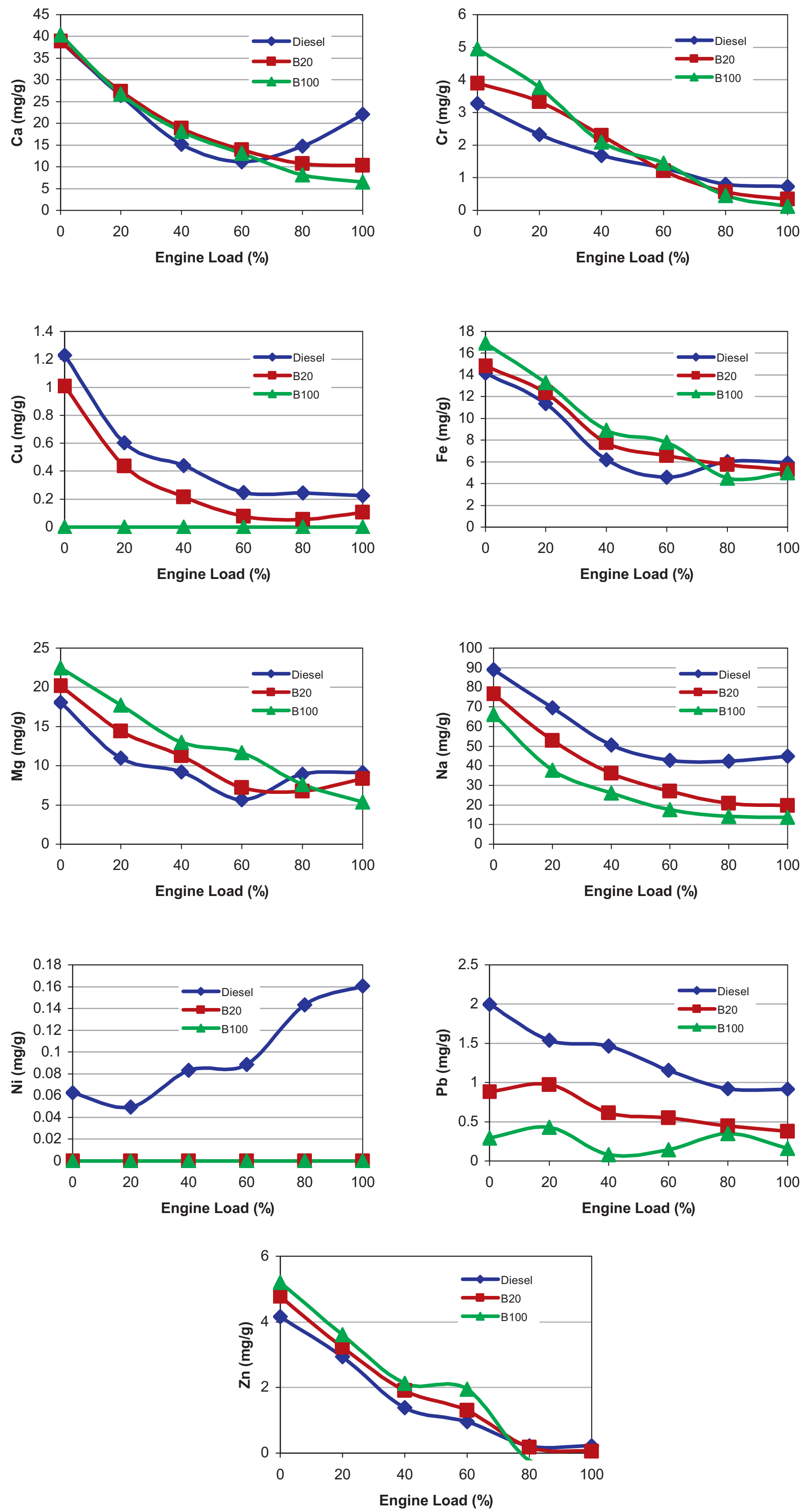


Fig. 5. Concentration of various metals in exhaust particulates with varying engine load at 1800 rpm.

decreasing up to 100% load. Some metals are found in excess in biodiesel's particulates, whereas some metals are found in excess in mineral diesel particulates. Usually metals, which are already present in the fuel as a constituent, are observed to be in the exhaust particulates in the same proportion. Metals that come from engine wear are not present in biodiesel exhaust particulate due to its self lubricating properties (leading to lesser wear) whereas these metals are present in diesel exhaust particulates. Mineral diesel used in the experiments was ordinary diesel (350 ppm Sulfur, BSIII) fuel available for distribution in non-metro cities, and has sufficiently high level of sulfur content in it. Sulfur has an important role in self-lubricating properties of diesel hence for ultra low sulfur diesel, these wear generated metal concentrations would be possibly even higher. [94]

4.1.2. Metal concentration in particulates with variation of engine speed at constant load

As the engine speed increases at constant load, concentration of the metals in the particulates also increase, because of lesser time available for the entire four-stroke process of an engine cycle to complete. Thus, with the increasing engine speed, time available for the combustion decreases and hence quality of combustion deteriorates leading to higher unburnt fuel coming out in the form of particulates. All the engine tests were carried out at 50% rated load at different engine speeds ranging from 1400 to 2400 rpm, in the present investigations. The results are shown in Fig. 6.

Calcium (Ca): Fig. 6 shows calcium concentration in particulates drawn from diesel, biodiesel and B20 exhaust at varying engine speed conditions. B100 exhaust shows highest Ca concentration throughout for the entire speed range. This is possibly due to lower calorific value of biodiesel, which leads to higher volumetric fuel consumption for the same load and speed conditions. Calcium is found in abundance in diesel (902.3 μg/g), biodiesel (721.2 μg/g) and lubricating oil (2046.8 μg/g).

Magnesium (Mg): Fig. 6 shows magnesium concentration in particulate drawn from diesel, biodiesel and B20 exhaust at varying engine speed conditions. B100 exhaust shows highest concentration of Mg and mineral diesel shows lowest. As the speed increases, difference between two curves goes on decreasing and for 2400 rpm, magnesium concentration for mineral diesel particulates is almost equal to the magnesium concentration from biodiesel particulates.

Iron (Fe): Fig. 6 shows iron concentration in particulates drawn from mineral diesel, B100 and B20 exhaust at varying engine speed conditions. Biodiesel shows higher concentration of iron in exhaust particulates. Mineral diesel shows lowest Fe concentration in the particulates amongst all. Lowest concentration of iron in the particulate is observed at 1700 rpm for all fuels.

Copper (Cu): Fig. 6 shows copper concentration in particulates drawn from mineral diesel, B100 and B20 exhaust at varying engine speed conditions. Diesel exhaust particulates show relatively very high level of copper concentration, B100 shows almost no trace of copper in the particulates. B20 shows copper concentration in particulates in between diesel and B100.

Chromium (Cr): Fig. 6 shows chromium concentration in particulates drawn from diesel, B100 and B20 exhaust at varying engine speed conditions at constant engine load.

Mineral diesel showed low Cr concentration in the exhaust particulates for lower engine speed however as the engine speed increases, difference between mineral diesel and B100 converges. For speeds greater than 2000 rpm, B100 gives lowest concentrations of Cr in the exhaust particulates. It seems that at higher engine speeds, fuel bound oxygen in biodiesel plays a role. Moreover self-lubricating properties of biodiesel also reduces contribution via wear of the engine components and keeps lubricating oil free from metal debris and reduces mixing of lubricating oil with fuel also.

Sodium (Na): Fig. 6 shows sodium concentration in particulate drawn from diesel, B100 and B20 exhaust at varying engine speed conditions. Diesel particulates show highest concentration of sodium among all fuels.

Nickel (Ni): Fig. 6 shows nickel concentration in particulates drawn from diesel, B100 and B20 exhaust at varying engine speed conditions at constant engine load. B20 shows a constant value for all the engine speeds. At 2000 and 2200 rpm, Ni was in non-detectable range for biodiesel particulates and even with increase in engine speed, it does not show any significant change in Ni concentration in particulates. Highest concentration of Ni in particulates is observed from mineral diesel.

Lead (Pb): Fig. 6 shows lead concentration in particulates drawn from diesel, B100 and B20 exhaust at varying engine speed conditions. Lowest Pb concentration is observed from Biodiesel and the highest concentration of Pb in particulates is observed from mineral diesel.

Zinc (Zn): Fig. 6 shows zinc concentration in particulates drawn from diesel, B100 and B20 exhaust at varying engine speed conditions. Zinc content is highest throughout the speed range for particulates from biodiesel since the Zn concentration is high in biodiesel (Table 7). This is found to be lowest in the particulates drawn from mineral diesel. Every graph for an individual fuel has its minimum value at 1700 rpm for the presence of Zn in the particulates. Rated speed for maximum load for this engine was 1800 rpm which gives an indication of most stable combustion at 1800 and 1700 rpm is the closest engine speed chosen for the present investigation.

There are several other studies carried out to observe the metal emissions in particulates from diesel engine. One such study was conducted by Sharma et al. [93] and they compared their results with some other studies available in open literature. Fe, Mg, Cr, Ni, Pb, Zn, Ca, Ba and Cd were measured in diesel particulate under various engine loading conditions. The experimental study showed that concentrations of Fe, Mg, Ca (crust elements) were much higher than those of Cr, Ni, Pb, Zn, Ba and Cd (anthropogenic elements). The metal concentrations determined in that study were compared with the results of Wang and Huang [95] (Fig. 7).

Brake specific fuel consumption of diesel engine decreases with increase in load and this is reflected in reduced emission of metals with increasing engine load [93]. Although the metal levels were generally lower (by a factor of 1–3) in this study compared to those reported by Wang and Huang [95] at full load, the relative emission trend from one metal to another was similar (Fig. 7).

Wang and Huang [95] reported that most of the emissions of metals in diesel particulates are from metals present in mineral diesel; therefore, it is desirable to compare metal contents in emission with metals present in mineral diesel. Fe, Mg, Cr, Ni, Zn, Pb, Ca, Ba, and Cd were measured in diesel (Fig. 8). The correlation coefficient between metal contents of diesel and DPM was found to be 0.73 [93]. Profile showed in Fig. 8 (between metal contents of diesel and DPM) suggests that concentration of metals in DPM is dependent on metal content in diesel; similar results were earlier reported by Wang and Huang [95].

The particles emitted from diesel engines are mainly aggregates of spherical carbon particles coated with organic and inorganic substances with the composition of the particles being predominantly 80–90% organic and inorganic carbon. Fig. 9 shows DPM composition at 70% load in the study compared by the composition given by Volkswagen [96] at 100% engine load. The other components in Fig. 9 include nitrogen, hydrogen, oxygen, and sulfur (estimated by difference). It can be seen that the broad composition of the particulates remains same with load and also when compared to the study of Volkswagen [96]. The particle composition of DPM exhaust emissions can vary greatly depending

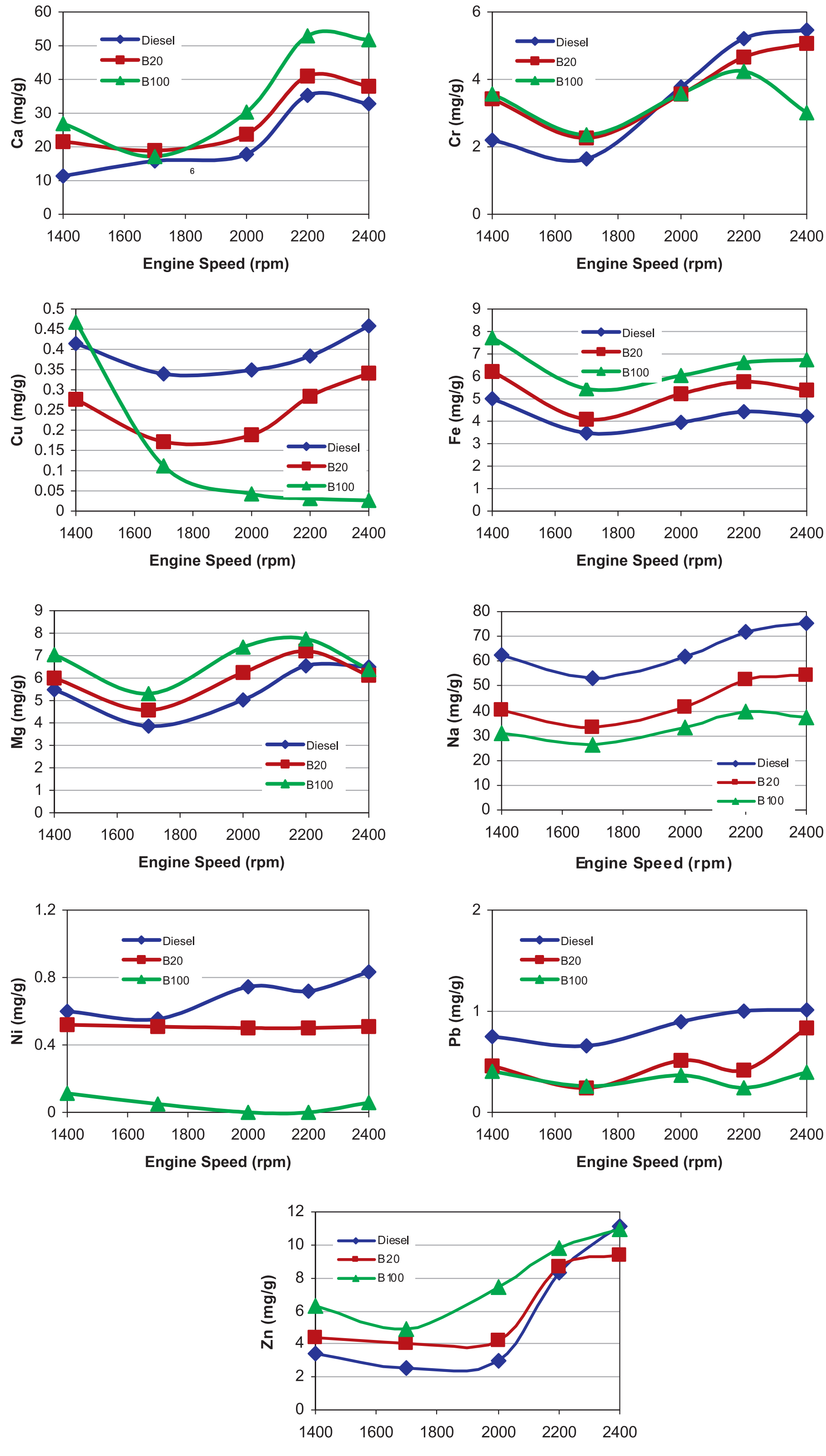


Fig. 6. Concentration of various metals in exhaust particulates with varying engine speeds at 50% rated load.

on the engine type, engine speed and load, fuel composition, lubricating oil type and emission control technology [97]. Therefore, there is a need to account for varying DPM composition while estimating (i) emission source profile, (ii) emission inventory and (iii) health implications of DPM [93].

4.2. BSOF estimations

Analysis for benzene soluble organic fraction (BSOF) of the particulate samples was carried out using ASTM test method D 4600-87 (ASTM, 2001) [98]. This method is also recommended by

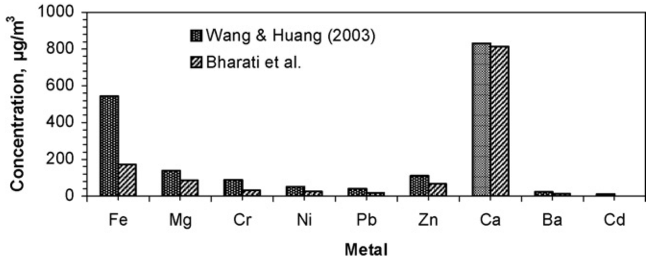


Fig. 7. Metal concentration in DPM at 100% engine load [93].

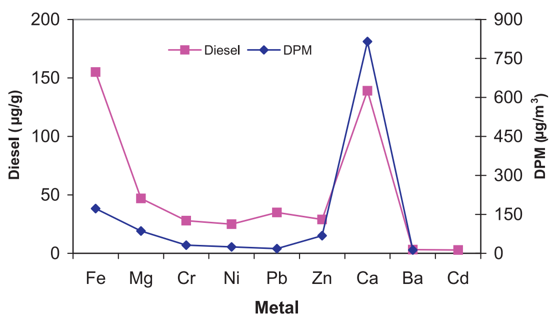


Fig. 8. Profile of metal content in diesel and DPM [93].

the National Institute of Occupational Safety and Health (NIOSH), USA to represent the toxic organic compounds in the particulate. This test method describes the sampling and gravimetric determination of BSOF of particulates.

4.2.1. BSOF with variable load at constant speed

As shown in the Fig. 10, BSOF percentage in the particulate matter for B100 is highest and for diesel is lowest among the three fuels tested. At no load condition, quality of combustion is relatively poor and the amount of unburned fuel coming out of the engine exhaust is high. BSOF of the particulates mainly consist of organic portion of the fuel itself and pyrolyticaly generated organic products formed during the process of soot formation [94].

As the engine load increases, BSOF of particulates decreases. At higher engine load, combustion efficiency is relatively superior hence amount of unburned fuel decreases thus amount of BSOF

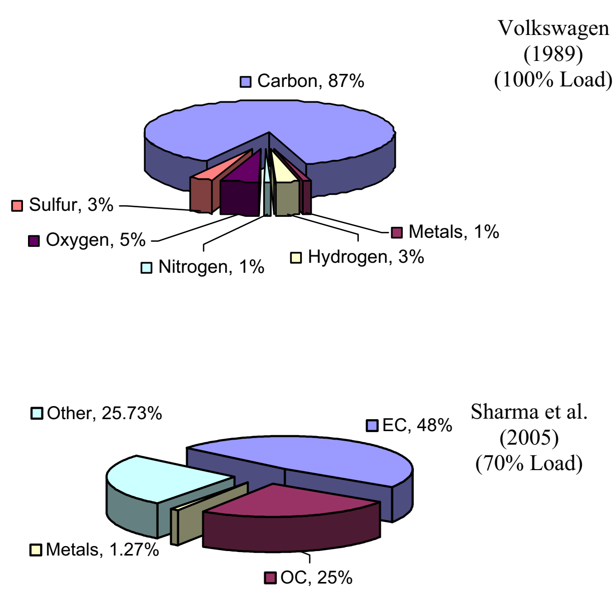


Fig. 9. Comparison of overall composition of DPM [93].

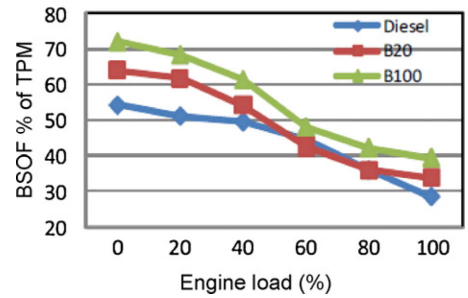


Fig. 10. BSOF percentage in terms of mass of total particulates with varying load conditions.

in particulates also decreases. Previous studies done on biodiesel exhaust showed a reduction in total mass of particulates [99]. Oxygen content of biodiesel mainly reduces the high carbon concentration part of particulates i.e. soot. Samples of diesel exhaust particulates are relatively darker in color and stickier than biodiesel exhaust. B20 seems like a good compromise between mineral diesel and biodiesel. BSOF percentage for B20 was more than mineral diesel and less than biodiesel. At higher engine loads, BSOF percentage from B20 was either very close or sometimes even less than mineral diesel.

Results of BSOF from previous studies carried out with mineral diesel are presented in Fig. 11 [93]. It can be observed that at idling condition, BSOF was about 67%, which gets lowered with increase in engine load. This can be explained by the fact that at idling, diesel fuel and lubricating oil undergo partial combustion or pyrolysis due to low temperature conditions prevailing in the combustion chamber. This leads to higher hydrocarbon emissions, which are detected as BSOF.

These results indicated that at low load conditions, the main component of the diesel particulates was soluble organic fraction. As the engine load increases, the proportion of soluble organic fraction decreases rapidly from 67% (at idling) to 24% (at full load). The results of BSOF in DPM are compared with the work of Ning et al. [100] (Fig. 11) who examined the soluble organic fraction using soxhlet extraction. It can be observed that pattern of variations in both the studies is comparable. The BSOF values in the present study are lower than Ning et al. [100] possibly due to difference in engines under investigation, and fuel composition.

4.2.2. BSOF with variable speed at constant load

As clearly visible from the Fig. 12, BSOF percentage for B100 is highest at all speeds and for mineral diesel, it is lowest. B20 showed the converging trend with relatively higher values than mineral diesel at low engine speed and almost similar values at higher engine speeds. As speed increases, BSOF percentage of particulates from mineral diesel, B20, and biodiesel increases. As speed increases, time available for air to be taken in during the induction

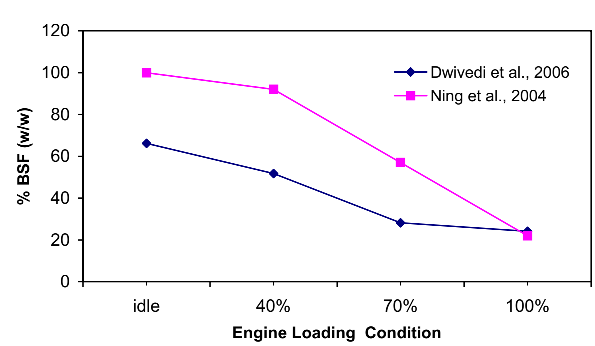


Fig. 11. Variation of BSOF from mineral diesel with engine load conditions [93].

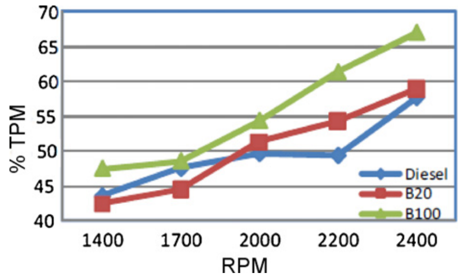


Fig. 12. BSOF percentage in terms of mass of total particulates with variable speed at constant load.

stroke, compression stroke, mixing of fuel with compressed air and ignition decreases, which increases the chances of fuel coming out unburnt or partially burnt hydrocarbons, in the form of BSOF [94].

4.3. Elemental and organic carbon in particulates

The results of measurement of elemental carbon (EC) and organic carbon (OC) in DPM are shown in Fig. 13.

It can be seen that at idling condition, total carbon was about 60% by weight, which gradually increased to 75% at 70% of rated load [93]. The EC also showed similar gradually increasing trend. The trend of OC was quite opposite. OC was 35% at idling, which was maximum and dropped down to 25% at 70% engine load. Since benzene soluble fraction is also an indicator of organic carbon, the trends in emission of BSOF (Fig. 11) and OC (Fig. 13) are quite similar with respect to engine load. This is an independent test that OC emissions decrease with increase in engine load.

4.4. Particulate size and number distribution using B100, B20, and mineral diesel

Since there is transportation of aerosol through pipes or tubes, there has to be some diffusion losses for the particulates since the measuring size range is between 5.6 and 560 nm. These diffusion losses are proportional to the length of the gas tube, and inversely proportional to the sample flow and independent of the tube inner diameter [99].

For the EEPS 3090,	Particle size	30 nm
	Length of the gas tube	3 m
	Sample flow rate	1 lpm
	Diffusion losses are	4%/m
	Therefore total losses approx	12%

All the data reported in this section here has been corrected for the diffusion losses, taking place in the transportation pipes. Particle size here represents, electrical mobility diameter, it does not exactly represent the diameter of the particle but it is quite close to its geometric diameter upon neglecting its shape.

The particle size and number distribution from the engine was measured at (i) constant engine speed (1800 rpm) at varying load and (ii) constant load (50% rated load) at varying engine speed and the results are reported here.

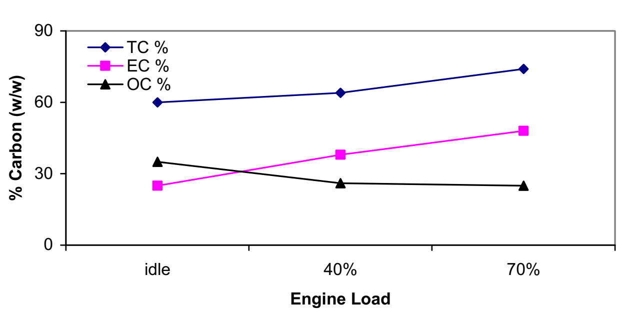


Fig. 13. Variation of EC and OC with engine loading condition [93].

4.4.1. Particulate size and number distribution: load variation at constant engine speed

Fig. 14 shows the particle concentration per unit volume flow rate of the exhaust for different size ranges of the particles varying with the variation of load on the engine. The units for particle concentration henceforth is # particles/cc. In this experimental study, three different fuels B20, biodiesel and mineral diesel have been used. Objective of the experiments was to study the effects of engine operating conditions i.e. for variation in load, on particle size and their number distribution for different fuel at constant operating speeds, emitted in diesel engine exhaust.

B20 showed highest particle concentration at no engine load and with the increase in load i.e. at 20% load, peak concentration decreased from 2.8 E + 08 to 1.5 E + 08. Peak particle concentration for B20 decreases steadily with increase in engine load. For B20, peak particle concentration with increase in load varies as follows: at no load 2.8 E + 08, at 20% load 1.5 E + 08, 40% load 1.3 E + 08, at 60% load 1.0 E + 08, at 80% load .8 E + 08, and at 100% load 3.4 E + 07. Also with increase in engine load, the diameter of the particle in highest number also increases continuously.

B100 exhaust shows highest particle concentration for most of the load varying driving conditions. Highest particle concentration for B100 is achieved at 60% load i.e. 3.05 E + 08. For B100, exhaust particle concentration first increases with increase in load i.e. at 20%, it shows higher particle concentration as compared with no load condition; again at 40% load, it decreases and at 60% load, it reaches its maximum value of all conditions. After 60%, at 80% and 100% load, it decreases gradually. However it can be noticed that biodiesel emits 30–40 nm particles in maximum number concentrations at almost all the loads.

For B100, peak particle concentration with increase in load varied as follows: at no load 2.0 E + 08, at 20% 2.9 E + 08, 40% load 2.3 E + 08, at 60% load 3.05 E + 08, at 80% load 2.6 E + 08, and at 100% load 1.8 E + 08.

Mineral diesel shows lowest peak particle concentration for low engine load conditions as load increases, B20 particle concentration comes very close to diesel particle concentration and for very high loads, B20 shows lower particle concentration than mineral diesel. Among the three fuels used, mineral diesel shows peak particle concentration for the largest particles among the three fuels. Up to 80% load, diesel shows a trend of decreasing peak particle concentration but at 100% load, suddenly peak particle concentration rises very sharply in the range of bigger size particles. Peak particle concentration with increase in load varied as follows: at no load 1.3 E + 08, at 20% 1.25 E + 08, 40% load 1.25 E + 08, at 60% load 7 E + 07, at 80% load 8 E + 07, and at 100% load 1.2 E + 08.

At no load, B20 exhaust showed exceptionally high particle concentration. Rate of decrease of particle concentration for B20 was highest and though it started from a very high concentration of particles at 40% load, it matched the peak particle concentration of mineral diesel. After 40% load, peak concentration of B20 exhaust particles and mineral diesel exhaust particles lie in the same plane or B20 was having lower values of peak particle concentration but peaks for B20 were shifted in left direction i.e. smaller particle concentration were high for B20 exhaust than mineral diesel exhaust.

For B100, particle concentration remains high throughout the load varying engine operating conditions with their peak values at lower particle size. Up to 40% load, peak particle concentration for mineral diesel remained very close to 34 nm range. For loads higher than 60% peak particle concentration shifted to bigger size particles, close to 80 nm range. Among the three fuels for all loads, depending on the engine operating range, mineral diesel

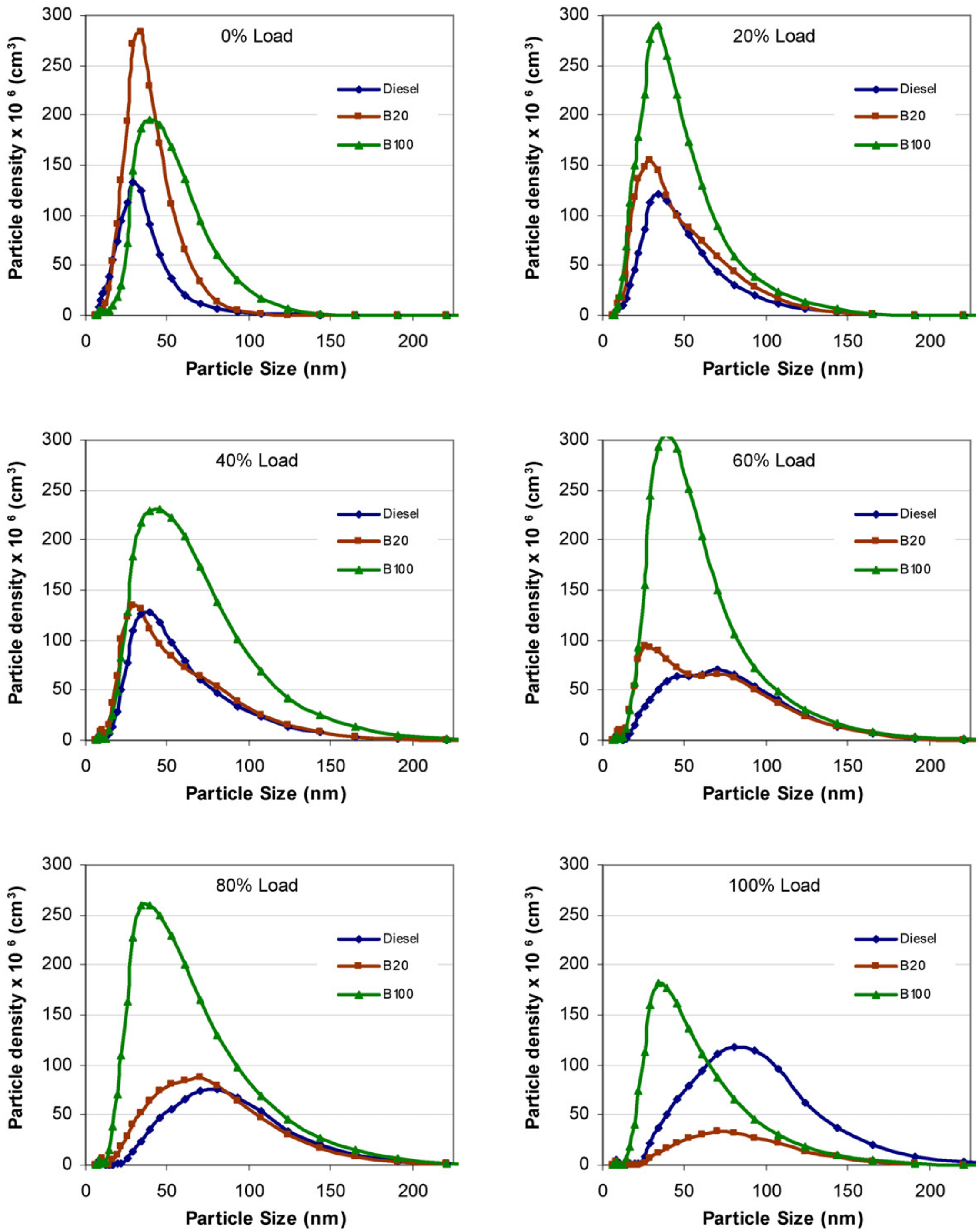


Fig. 14. Particle size vs. number per unit volume (/cm^3) at rated speed 1800 rpm for varying load conditions (no load, 20% load, 40% load, 60% load, 80% load, 100% rated load).

exhaust showed peak concentrations for biggest size particles i.e. diesel particle number peak values were always shifted in the right direction.

4.4.2. Particulate size and number distribution: Speed variation at constant engine load

To study the effect of speed variation on particle size and number distribution, various engine operating speeds have been chosen. Engine was operated at these operating speeds for some time to achieve stabilization so that repeatability of experiments can be ensured. At these operating speeds, engine was operated at constant load using different fuels in order to compare the effects of engine operating speeds on particulate formation with different fuels.

A fuel which gives very low particle concentration at low engine speeds but very high particle concentration at high engine speeds cannot be recommended as a good fuel [94]. Similarly particle size distribution very much depends upon nature of fuel and its response to engine operating conditions.

Fig. 15 shows the particle size and number distribution per unit volume with the variation of operating speed of the engine at constant engine load of 50% rated load. In this experimental study, three

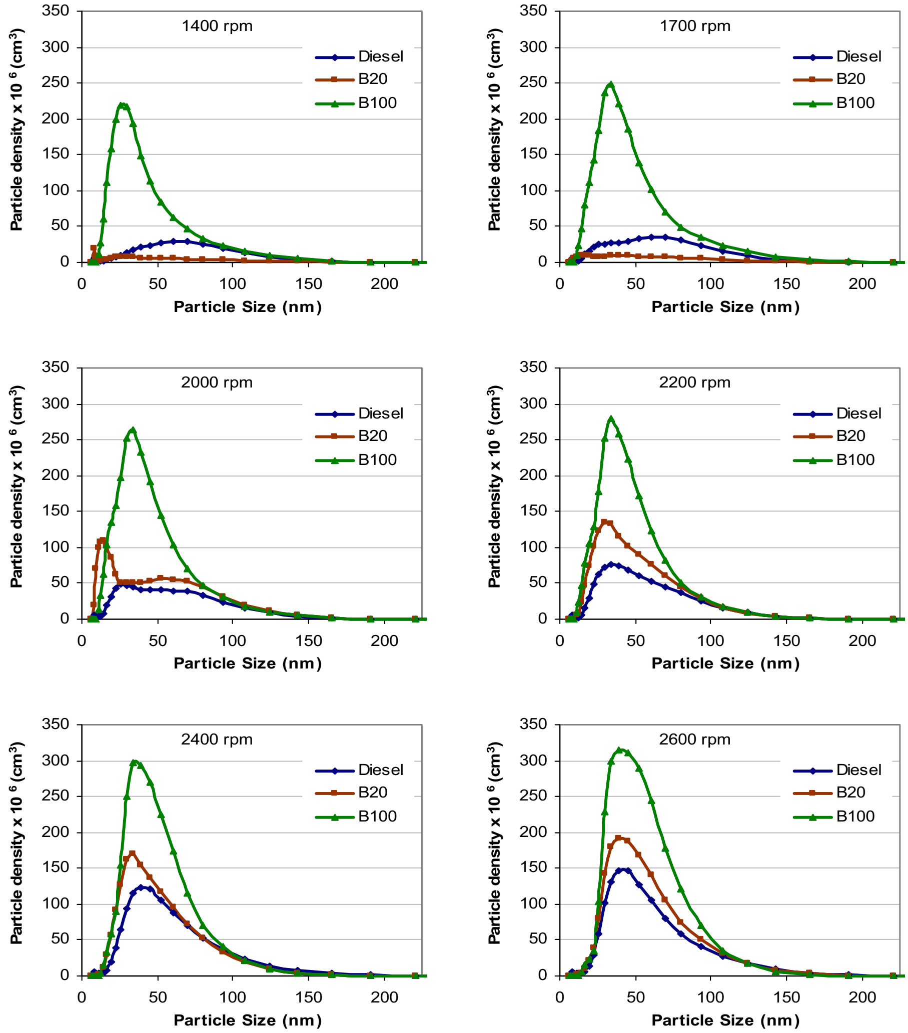


Fig. 15. Particle size and number distribution at 50% rated engine load for different engine operating speeds.

different fuels B20, biodiesel and mineral diesel have been used. Objective of the experiments was to study the effects of engine operating conditions (i.e. with variation in engine speed at constant load), on particle size and their number distribution for different fuels.

B20 gives very low particle concentration at low engine speeds, i.e. for 1400 and 1700 rpm, B20 exhaust particle concentration is barely visible in the graph. Between 1700 and 2000 rpm, particle concentration for B20 exhaust increases 10 times i.e. peak particle concentration at 1700 rpm is 1.0 E + 07 and peak particle concentration at 2000 rpm is 1.0 E + 08. After 2000 rpm, peak particle concentration increases gradually. Peak particle concentration with increase in speed varies as follows: at 1400 rpm 1.9 E + 07, at 1700 rpm 1.0 E + 07, at 2000 rpm 1.09 E + 08, at 2200 rpm 1.35 E + 08, at 2400 rpm 1.7 E + 08, and at 2600 rpm 1.92 E + 08.

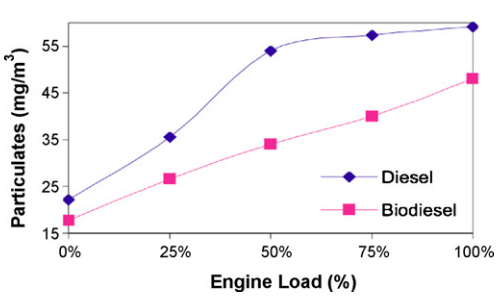


Fig. 16. Variation in particulate emission with engine load.

Biodiesel shows highest peak particle concentration for all speeds. As speed increased, peak particle concentration also increased gradually. Peak particle concentration for B100 exhaust always occurs in 30–40 nm size range. At low engine speeds, peak particle concentration for B100 exhaust was relatively higher than B20 or mineral diesel exhaust but as the speed increases, difference between these curves decreased i.e. at 1400 rpm, biodiesel showed 10 times more peak particle concentration than any other fuel used whereas at 2600 rpm this difference decreased to only 2 times. Peak particle concentration (for B100) with increase in speed varied as follows: at 1400 rpm 2.19 E + 08, at 1700 rpm 2.49 E + 08, at 2000 rpm 2.64 E + 08, at 2200 rpm 2.79 E + 08, at 2400 rpm 2.97 E + 08, and at 2600 rpm 3.15 E + 08.

Mineral diesel showed lowest peak particle concentration except for low engine speed operating conditions. Other than that, mineral diesel exhaust curve always remained below the curves for B20 and B100. For low engine speeds, mineral diesel did not show any visible peaks and the particles appeared to be in a more evenly size distributed form. For mineral diesel, peak particle concentration with increase in speed varied as follows: at 1400 rpm 2.9 E + 07, at 1700 rpm 3.5 E + 07, at 2000 rpm 4.8 E + 07, at 2200 rpm 7.6 E + 07, at 2400 rpm 1.24 E + 08, and at 2600 rpm 1.47 E + 08.

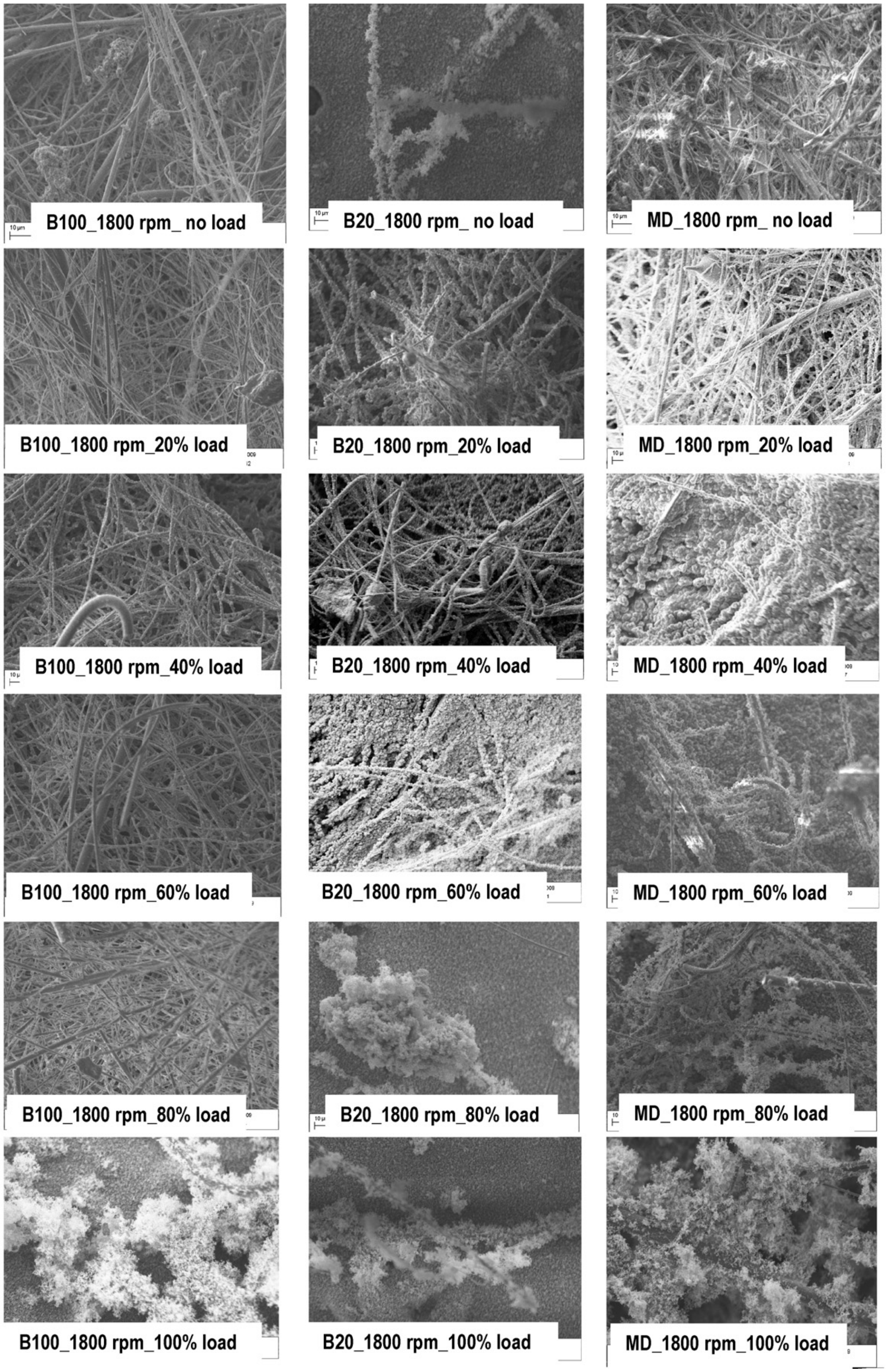


Fig. 17. Scanning Electron Micrographs at rated speed (1800 rpm) for varying load conditions (no load, 20% load, 40% load, 60% load, 80% load, 100% rated load).

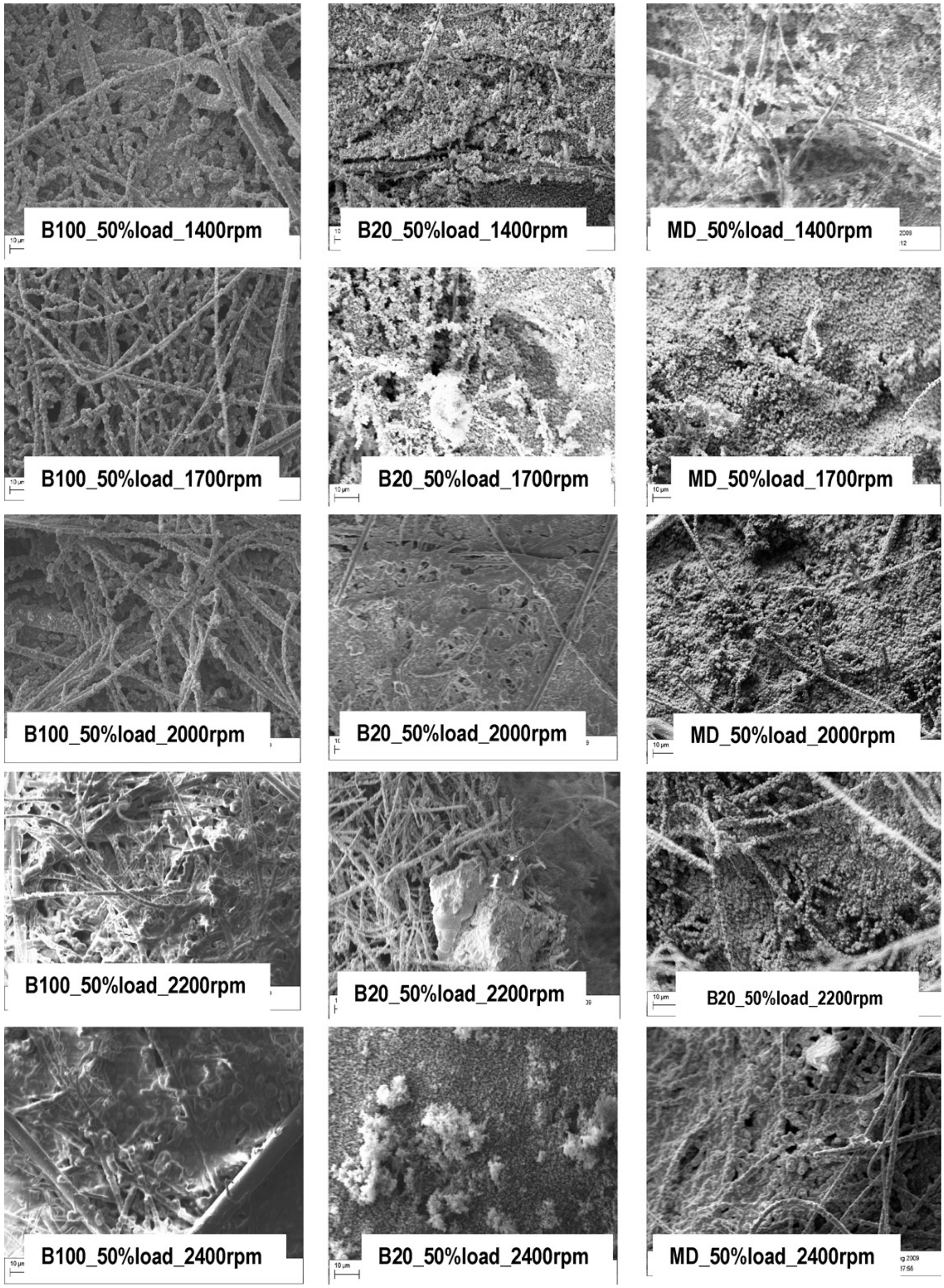


Fig. 18. Scanning Electron Micrographs at 50% rated engine load for different engine operating speeds.

Objectives of another study by Dwivedi et al. [101] was to examine particulate emission in diesel exhaust and biodiesel blend (B20) exhaust under varying engine load conditions. Fig. 16 shows variations of particulate emission under varying engine loads for diesel and B20 fuel at constant engine speed. Shobokshy [102] and Sharma et al. [93] have reported that particulate concentration increases with increased engine load; the same trend is obtained in the study by Dwivedi et al. [101] for both the fuels (Fig. 16). However, it is noteworthy that particulate emission is higher in diesel exhaust (22 to 59 mg/m^3) than B20 exhaust (17–48 mg/m^3). Studies by Sharp [103] and Wedel [12] established that a B20 blend (approximately 2% oxygen for RME-20) reduces particulate by approximately 30% compared to particulate in the DE. In another recent study, three test fuels namely low sulfur diesel fuel (BP15), a pure soybean methyl-ester biodiesel fuel (B100), and a synthetic Fischer–Tropsch fuel (FT) were tested. B100 produced the highest PM emissions (concentration of 1.2 E + 7/cm^3), but generally had the smaller particle mean diameter (around 38 nm) [104,105].

Fig. 16 shows that rate of increase (with increasing load) of particulate emission is lower for B20 exhaust. This lower increase in particulate concentration in B20 exhaust can be attributed to (i) higher oxygen content in B20 and (ii) lower C/H ratio; in B20 C/H ratio 6.53 compared to diesel 6.82 [106,107] and (iii) near absence of sulfur and aromatic content of biodiesel.

4.5. Particulate surface morphology

4.5.1. Variation in load at rated rpm for mineral diesel, B20 and B100 samples:

SEM images for all particulate samples were taken at 1000× magnification (Fig. 17). Filters were exposed for the same (approximately) duration through filter assembly connected in partial dilution tunnel.

SEM images at no load for B100 shows that at no load a very fine layer of agglomerates has accumulated. In terms of total particle accumulation, at no load, B100 showed higher particle accumulation than mineral diesel and B20. B100 particulate agglomeration decreases sharply between no load and 20% load and it shows lower agglomeration than B20 and mineral diesel. B20 and mineral diesel shows comparable particle agglomeration. For 40–60% load operating condition B100 particulate depositions decrease rapidly whereas mineral diesel and B20 particulate deposition increase. At these operating conditions, mineral diesel shows highest particulate deposition and biodiesel (B100) shows lowest particulate deposition. Biodiesel exhaust particulate show least size granular structure whereas mineral diesel shows biggest size granular structure. At 80% load operating condition, biodiesel (B100) shows least particle agglomerations compared to mineral diesel and B20. At full load condition, B100 particle accumulation rises sharply but still remains lower than mineral diesel and B20. Mineral diesel shows very big size particle agglomerates compared to B20 and B100. Also, at 100% load, the structure of particulates changes from granular structures to flake-like structure. It can be seen that at full load, B20 exhibits minimum amount of particulate accumulation.

For B20, particle accumulations decreases as load increases till 40% load and after that it rises again. At high load conditions, if loads are further increased, bigger size particles can be easily seen on the filter deposits. For mineral diesel, particle accumulation rises as load increases. For mineral diesel, as load increases size of particles also increases.

Among the three fuels used here, B100 showed highest particle accumulation at no load but least particle accumulation as load increases. At same load operating conditions, mineral diesel showed biggest size particles for all load conditions and maximum particle accumulation for all loads except for very low load operating conditions.

4.5.2. Variation in speeds at 50% load for mineral diesel, B20 and B100 samples

SEM images for all particulate samples were taken at 1000× magnification (Fig. 18). Filters were exposed for the same (approximately) duration through filter assembly connected in partial dilution tunnel.

A common trend for all fuels is that as engine speed increases, SEM images looks more continuous and homogeneous in nature and number of small size particles increases rapidly along with total number of particles.

Among B100, B20 and mineral diesel, total particle accumulation is maximum for mineral diesel i.e. filter sample looks more filled with particulates. In other words, mass of total particulate seem higher for mineral diesel samples.

At 1400 rpm, biodiesel shows bigger size particle agglomerates, whereas mineral diesel shows smaller size particle agglomerates in flaky form. B100 shows maximum particle deposition for 1400 rpm. At 1700 rpm, total particulate accumulation is maximum in case of mineral diesel and minimum in case of biodiesel. Biodiesel still shows larger particle agglomerates than mineral diesel. At 2000, 2200 and 2400 rpm, total particulate accumulation is maximum in case of mineral diesel exhaust particulate, whereas biodiesel still shows bigger size particle agglomerates than mineral diesel. B20 particulate accumulation is comparable to biodiesel whereas its particle size is more close to mineral diesel. Biodiesel particulates at 2400 rpm looks wetter compared to mineral diesel particulates.

SEM images for B100 and B20 shows granular structure particulates with bigger grain size compared to mineral diesel.

5. Conclusions

This study was carried out to characterize the engine exhaust particulate emissions from biodiesel fuelled engine vis-à-vis mineral diesel. Experiments done to investigate metal concentrations showed that some metals were excess in mineral diesel and some were is biodiesel, metals like Ca, Mg, Fe, Zn were found in higher quantities in biodiesel exhaust for almost all operating conditions where as metals like Cu, Pb, Cr, Ni, Na were found in excess in mineral diesel exhaust particulate. The major results from the study showed that metals that come from engine wear were not present in biodiesel exhaust particulate due to its self lubricating properties. It was clearly visible that metals coming out in excess in mineral diesel exhaust particulates were toxic in nature, and some of these toxic metals were not originally present in the mineral diesel but they came from the engine wear or due to lubrication failure/combustion of lubricating oil at very high temperatures. At high speeds or at high loads, biodiesel performance remained consistent and did not deteriorate as it was observed in case of mineral diesel.

The organic content in diesel exhaust measured through BSOF and organic carbon both decreased with increase in engine load, from maximum at idling condition. However, the elemental carbon increased with increase in engine load. Samples collected of mineral diesel exhaust were relatively darker in color and stickier than biodiesel exhaust. Biodiesel and its blends gave more BSOF in engine exhaust particulates than mineral diesel at all operating conditions. At higher engine loads, BSOF percentage from B20 was either closer to or even lesser than mineral diesel. Experiments done regarding BSOF content in biodiesel showed that biodiesel and its blends gave more BSOF in engine exhaust particulate matter than mineral diesel at all operating conditions, but B20 values were very close to mineral diesel results. There was a net increase in BSOF for B20 fuel as compared to mineral diesel, however biodiesel is non-toxic, hence the increased level of soluble organic fraction may not be viewed as hazardous [108]. However, hazardous nature of biodiesel exhaust needs further investigations by speciating organic species in biodiesel exhaust. This necessitates that speciation of organic compounds is done for both the fuel exhausts to clearly establish comparative organic toxicity.

Biodiesel gave higher number of smaller particles in its exhaust than mineral diesel; combined figures of all size particles were also higher in case of biodiesel. Peak particle concentrations for biodiesel were shifted towards smaller size particles. Whereas, B20 delivered better performance compared to B100, particle concentrations for B20 were comparable to mineral diesel and for some operating conditions it was even better than mineral diesel. As load increases, B20 emission performance in terms of particle concentrations improves very rapidly and even surpasses mineral diesel emission performance. For all engine operating speeds, biodiesel always showed highest particle concentration whereas B20 gave mixed results. For all operating conditions (both load and speed),

peak particle concentrations for B100 and B20 were always in lower side, i.e. high small size particle concentrations.

Scanning electron microscope (SEM) images for B100 and B20 showed granular structure particulates with bigger grain size compared to mineral diesel. Among B100, B20 and mineral diesel, total particle accumulation was maximum for mineral diesel. In other words, mass of total particulates seem higher for mineral diesel samples.

References

[1] Krzyzanowski M, Kuna-Dibbert B, Schneider J. Health Effects of Transport-Related Air Pollution. World Health Organization; 2005.

[2] Kunzli N, Kaiser R, Medina S, Studnicka M, Chanel O, Filliger P, et al. Public-health impact of outdoor and traffic-related air pollution: a European assessment. Lancet 2000;356:795–801.

[3] Schlesinger RB, Kunzli N, Hidy GM, Gotschi T, Jerrett M. The health relevance of ambient particulate matter characteristics: coherence of toxicological and epidemiological inferences. Inhal Toxicol 2006;18:95–125.

[4] Dockery DW, Pope CA, Xu X, Splenger JD, Ware JH, Fay ME, et al. An association between air pollution and mortality in six U.S. cities. J Med 1993;329:1753–9.

[5] Chow JC, Watson JG. Guidelines on Speciated Particulate monitoring. Research Triangle Park: USEPA, Office of Air Quality Planning and Standards; 1998.

[6] Kumar A, Patil RS, Nambi KSV. Source apportionment of suspended particulate matter at two traffic junctions in Mumbai, India. Atmos Environ 2001;35:4245–51.

[7] CPCB, 1995. Air Pollution and its Control. Newsletter, April 1995, Central Pollution Control Board, Delhi.

[8] California Environmental Protection Agency (CAL EPA), 1998. Part B: Health Risk Assessment for Diesel Exhaust, Proposed Identification of Diesel Exhaust as a Toxic Air Contaminant. Office of Environmental Health Hazard Assessment (OHEEA).

[9] EPA Clean Air Scientific Advisory Committee (CASAC), 2000. Review of EPA's Health Assessment Document for Diesel Emissions. Clean Air Scientific Advisory Committee (CASAC). February, 2000a, EPA 600/8-90/057D.

[10] USEPA, 1995. Air Quality Criteria for Particulate Matter, Vol. II. External review draft EPA/600/AP-95/001b, U.S. Environmental Protection Agency, Office of Research and Development, Washington DC.

[11] Crebelli R, Fuselli S, Conti G, Conti L, Carere A. Mutagenicity spectra in bacterial strains of airborne and engine exhaust particulate extracts. Mut Res 1991;261:237–48.

[12] Wedel RV. Marine Biodiesel in Recreational Boats, CytoCulture International, Inc. Point Richmond, CA, Second Edition, and April 22, 1999. Marine Biodiesel and Education Project for San Francisco Bay and Northern California. Prepared for the National Renewable Energy Laboratory U.S. Department of Energy, 1999.

[13] Johnson J H, Bagley ST, Gratz LD, Leddy DG. A review of diesel particulate control technology and emission effects. SAE Transactions 1994; ISSN 0096-736X, 103:210–244.

[14] Baumgard KJ, Johnson JH. The effect of low sulfur fuel and a ceramic particle filter on diesel exhaust particle size distributions. SAE Trans 1992;101:691–9.

[15] Kittelson DB. Engines and nanoparticles: a review. J Aerosol Sci 1998;29:575–88.

[16] Williams PT. The role of lubricating oil in diesel particulate and particulate PAH emissions. SAE Technical Paper No. 87084, 1987.

[17] Bagley ST, Baumgard KJ, Gratz L D, Johnson JH, Leddy DG. Characterization of fuel and aftertreatment device effects on diesel emissions. Health effects institute research report number 76; 1996.

[18] Andrews GE, Abbass MK, Abdelhalim S, Farrar KJ, Ghazikhani M, Ounzain A, et al. Unburned liquid hydrocarbons using differential temperature hydrocarbon analysers. Soc Auto Eng 2000, 2000-01-0506.

[19] Bertoli C, Del GN, Caprotti R, Smith AK. The influence of automotive diesel back end volatility and new fuel additive technology on regulated emissions. Inst Mech Eng 1991 [C427/34/218].

[20] Dobbins RA, Fletcher RA, Benner BA, Hoeft S. Polycyclic aromatic hydrocarbons in flames, in diesel fuels and in diesel emissions. Combust Flame 2006;144:773–81.

[21] Akihama K, Takatori Y, Inagaki S, Dean AM. Mechanism of the smokeless rich diesel combustion by reducing temperature. Soc Auto Eng 2001 [2001-01-0655].

[22] Particulate Emissions from Vehicles by Peter Eastwood; 2008, p. 45.

[23] Dale RT, Kenth IS. Soot process in compression ignition engine. Prog Energy Combust Sci 2006;33:272–309.

[24] Liang F, Lu M, Birch ME, Keener TC, Liu Z. Determination of polycyclic aromatic sulfur heterocycles in diesel particulate matter and diesel fuel by gas chromatography with atomic emission detection. J Chromatogr A 2006;1114:145–53.

[25] Glassman I. Combustion. San Diego: Academic Press; 1996.

[26] Smith OI. Fundamentals of soot formation in flames with application to diesel engine particulate emissions. Prog Energy Combust Sci 1981;7:275–91.

[27] Haynes BS. In: Bartok W, Sarofim AF, editors. Fossil Fuel Combustion. New York: Wiley; 1991. p. 261–326.

[28] Haynes BS, Wagner HG. Soot formation. Prog Energy Combust Sci 1981;7:229–73.

[29] Bryce D, Ladommatos N, Xiao Z, Zhao H. Investigating the effect of oxygenated and aromatic compounds in fuel by comparing laser soot measurements in laminar diffusion flames with diesel-engine emissions. J Inst Energy 1999;72:150–6.

[30] Randy Vander Wal L, Aaron Tomasek J. Soot oxidation: dependence upon initial nanostructure. Combust Flame 2003;134:1–9.

[31] Juhun S, Mahabubul A, Landré B, Unjeong K. Examination of the oxidation behavior of biodiesel soot. Combust Flame 2006;146:589–604.

[32] Lee KO, Cole R, Sekar R, Choi MY, Zhu J, Kang J, et al., Detailed characterization of morphology and dimensions of diesel particulates via thermophoretic sampling. SAE Paper 2001-01-3572; 2001.

[33] Bruce CW, Stromberg TF, Gurton KP, Mozer JB. Transspectral absorption and scattering of electromagnetic radiation by diesel soot. Appl Optics 1991;30(12):1537–46.

[34] Tree DR, Foster DE. Optical measurements of soot particle size, number density, and temperature in a direct injection diesel engine as a function of speed and load. SAE Paper 940270; 1994.

[35] Pinson JA, Ni T, Litzinger TA. Quantitative imaging study of the effects of intake air temperature on soot evolution in an optically-accessible D.I. diesel engine. SAE Paper 942044; 1994.

[36] Ladommatos N, Zhao H. A guide to measurement of flame temperature and soot concentration in diesel engines using the two-colour method. Part 1: principles. SAE Paper 941956; 1994.

[37] Hare CT. Characterization of Diesel Engine Gaseous Particulate Matter, Final Report, prepared by South West Research Institute contract no. 68-02-1977; 1977.

[38] Lowenthal DH, Zielinska B, Chow JC, Watson JG. Characterization of heavy-duty diesel vehicle emissions. Atmos Environ 1994;28(4):731–43.

[39] Springer KJ. Characterization of Sulfate, Odor, Smoke, POM and particulates from Light duty and Heavy duty Diesel Engines- Part IX, prepared by South West Research Institute, EPA/460/3-79/007; 1997.

[40] Norbeck JM, Durbin TD, Truex TJ. Measurement of Primary Particulate Matter Emissions from light duty Motor Vehicles. Center for Environmental research and technology, college of engineering. Riverside, CA: University of California; 1998.

[41] Warnatz J, Maas U, Dibble RW. Combustion: Physical and Chemical Fundamentals, Modeling and Simulation, Experiments, Pollutant Formation. Berlin: Springer; 1999.

[42] Pope CA. Epidemiology of fine particulate air pollution and human health: biologic mechanisms and who's at risk? Environ Health Perspect 2000;108(4):713–23.

[43] International Life Sciences Institute (ILSI). The relevance of the rat lung response to particle overload for human risk assessment, in ILSI Risk Science Institute Workshop, (ed. D.E. Gardner), Inhalation Toxicology 2000;12(1–2):1–148.

[44] U.S. EPA. Health assessment document for diesel engine exhaust. EPA Report No. 600/8-90-057F; 2002.

[45] U.S. EPA. Clean Air Act, 1990.

[46] Integrated Risk Information System (IRIS) (2003). Diesel engine exhaust. http://www.epa.gov/iris/subst/0642.htm.

[47] Mauderly JL, Griffith WC, Henderson RF, Jones RK, Mc Clellan RO. Evidence from animal studies for the carcinogenicity of inhaled diesel exhaust. In: Howard PC, editor. Nitroarenes. New York: Plenum Press; 1990. p. 13.

[48] Mauderly JL. Diesel exhaust. In: Lippmann M, editor. Environmental Toxicants – Human Exposures and their Health Effects. New York: Van Nostrand Reinhold; 1992. p. 19–62.

[49] Heinrich U, Fuhst R, Rittinghausen S. Chronic inhalation exposure of Wistar rats and two different strains of mice to diesel engine exhaust, carbon black, and titanium dioxide. Inhal Toxicol 1995;7:533–56.

[50] Nikula KJ, Snipes MB, Barr EB. Comparative pulmonary toxicities and carcinogenicities of chronically inhaled diesel exhaust and carbon black in F344 rats. Fundam Appl Toxicol 1995;25:80–94.

[51] Sjogren M, Li H, Banner C, Rafter J, Westerholm R, Rannug U. Influence of physical and chemical characteristics of diesel fuels and exhaust emissions on biological effects of particle extracts: a multivariate statistical analysis of ten diesel fuels. Chem Res Toxicol 1996;9:197–207.

[52] Valavanidis A, Salika A, Theodosopoulou A. Generation of hydroxyl radicals by urban suspended particulate air matter. The role of iron ions. Atmos Environ 2000;34:2379–86.

[53] Wu WD, Samet JM, Ghio AJ, Devlin RB. Activation of the EGF receptor signaling pathway in airway epithelial cells exposed to Utah Valley PM. Am J Physiol-Lung C 2001;281:483–9.

[54] Gilmour PS, Brown DM, Lindsay TG, Beswick PH, MacNee W, Donaldson K. Adverse health-effects of PM(10) particles – involvement of iron in generation of hydroxyl radical. Occup Environ Med 1996;53:817–22.

[55] Smith KR, Aust AE. Mobilization of iron from urban particulates leads to generation of reactive oxygen species in vitro and induction of ferritin synthesis in human lung epithelial cells. Chem Res Toxicol 1997;10: 828–34.

[56] Jimenez LA, Thompson J, Brown DA, Rahman I, Antonicelli F, Duffin R, et al. Activation of NF-kappaB by PM(10) occurs via an iron-mediated mechanism in the absence of IkappaB degradation. Toxicol Appl Pharmacol 2000;166:101–10.

[57] Pepelko WE, Peirano WB. Health effects of exposure to diesel engine emissions. J Am Coll Toxicol 1983;2:253–306.
[58] Madden MC, Richards JH, Dailey LA, Hatch GE, Ghio AJ. Effect of ozone on diesel exhaust particle toxicity in rat lung. Toxicol Appl Pharmacol 2000;168:140–8.
[59] Schwartz DA. Does inhalation of endotoxin cause asthma? Am J Respir Crit Care Med 2001;163:305–13.
[60] Arbour NC, Loren E, Schutte BC, Zabner J, Kline JN, Jones M, et al. TLR4 mutations are associated with endotoxin hyporesponsiveness in humans. Nat Genet 2000;25:187–91.
[61] Leikauf GD, Mc Dowell SA, Gammon K, Wesselkamper SC, Bachurski CJ, Puga A, et al. Prows DR. Functional genomics of particle-induced lung injury. Inhal Toxicol 2000;12(3):59–73.
[62] Prows DR, Leikauf GD. Quantitative trait analysis of nickel-induced acute lung injury in mice. Am J Respir Cell Mol Biol 2001;24:740–6.
[63] McDowell SA, Gammon K, Bachurski CJ, Wiest JS, Leikauf JE, Prows DR, et al. Differential gene expression in the initiation and progression of nickel-induced acute lung injury. Am J Respir Cell Mol Biol 2000;23:466–74.
[64] Johnston CJ, Finkelstein JN, Mercer P, Corson N, Gelein R, Oberdorster G. Pulmonary effects induced by ultrafine PTFE particles. Toxicol Appl Pharmacol 2000;168:208–15.
[65] Hunter DD, Undem BJ. Identification and substance P content of vagal afferent neurons innervating the epithelium of the guinea pig trachea. Am J Respir Crit Care Med 1999;159:1943–8.
[66] Park JH, Gold DR, Spiegleman DL, Burge HA, Milton DK. House dust endotoxin and wheeze in the first year of life. Am J Respir Crit Care Med 2001;163:322–8.
[67] Hauser R, Eisen EA, Pothier L, Christiani DC. A prospective study of lung function among boilermaker construction workers exposed to combustion particulates. Am J Ind Med 2001;39:454–62.
[68] ATSDR. Tox FAQs for Polycyclic Aromatic Hydrocarbons (PAHs). Atlanta, GA: Agency for Toxic Substances and Disease Registry; 1996.
[69] Demirbas A. Biodiesel production from vegetable oils via catalytic and non-catalytic supercritical methanol transesterification methods. Prog Energy Combust Sci 2005;31(5–6):466–87.
[70] Desjardins-Pepiot P, Pitsch H, Malhotra R, Kirby RS, André Boehman L. Structural group analysis for soot reduction tendency of oxygenated fuels. Combust Flame 2008;154:191–205.
[71] Geller DP, Goodrum JW. Effects of specific fatty acid methyl esters on diesel fuel lubricity. Fuel 2004;83(17–18):2351–6.
[72] Zhao X, Ren M, Liu Z. Critical solubility of dimethyl ether (DME + diesel fuel and dimethyl carbonate (DMC) + diesel fuel. Fuel 2005;84:2380–3.
[73] Vertin KD, Ohi JM, Naegeli DW, Childress KH, Hagen GP, Mccarthy CI, et al. Methyl and methyl diesel blended fuels for use in compression ignition engines. Soc Auto Eng 1999 [1999-01-1508].
[74] Labeckas G, Slavinskas S. Performance and exhaust emission characteristics of direct-injection diesel engine when operating on shale oil. Energy Convers Manag 2005;46:139–50.
[75] deMan JM, Tie F, deMan L. Formation of short chain volatile organic acids in the automated AOM method. J Am Oil Chem Soc 1987;64:993–6.
[76] McCormick RL, Ratcliff M, Moens L, Lawrence R. Several factors affecting the stability of biodiesel in standard accelerated tests. Fuel Process Technol 2007;88:651–7.
[77] Yeh LI, Rickeard DJ, Schlosberg DH, Duff JCL, Caers RF, Bateman JR. Oxygenates: An Evaluation of Their Effects on Diesel Emissions, 2001-01-2019; 2001.
[78] Litzinger T, Stoner M, Hess H, Boehman A. Effects of oxygentade blending compounds on emissions from a turbo charged direct injection diesel engine. Int J Engine Res 2000;1:57–70.
[79] Suppes GJ, Lula CJ, Burkhart ML, Swearingen JD. Type Performance of Fischer-Tropsch Liquids (Ftl) in Modified Off-Highway Diesel Engine Test Cycle, 1999-01-1474; 1999.
[80] Sidhu S, Graham J, Striebich R. Semi volatile and particulate emissions from combustion of alternative diesel fuels. Chemosphere 2001;42:681–90.
[81] Lapuerta M, Armas O, Ballesteros R, Fernandez J. Diesel emissions from biofuels derived from Spanish potential vegetable oils. Fuel 2005;84:773–80.
[82] Bechtold RL, Timbario TJ, Miller MT, Urban C. Performance and emissions of a DDC 8V 71 transit bus engine using ignition improved methanol and ethanol. Soc Auto Eng 1991:912356.
[83] Grimaldi CN, Postrioti L, Battistoni M, Millo F. Common Rail HSDI diesel engine combustion and emissions with fossil/bio derived fuel blends. Soc Auto Eng 2002, 2002-01-0865.
[84] Romig C, Spataru A. Emissions and engine performance from blends of soya and canola methyl esters with ARB#2 diesel in a DDC6V92TA MUI engine. Bioresour Technol 1996;56:25–34.
[85] Trapel E, Mayer C, Schulz C, Roth P. Effects of bio diesel injection in a DI diesel engine on gaseous and particulate emission. Soc of Auto Eng 2005, 2005-01-2204.
[86] Gonzalez DMA, Piel W, Asmus T, Clark W, Garback J, Liney E, et al. Oxygantes screening for advanced petroleum based diesel fuels: part 2 the effects of oxygenate blending compounds on exhaust emissions. Soc Auto Eng 2001, 2001-01-3632.
[87] Miyamoto N, Ogawa H, Nurun NM, Obata K, Arima T. Smokeless low NOx, high thermal efficiency, and low noise diesel combustion with oxygenated agents as main fuel. Soc Auto Eng 1998;980506.
[88] Rakopoulos CD, Antonopoulos KA. Multi zone modeling of diesel engine fuel spray development with vegetable oil, bio diesel or diesel fuels. Energy Convers Manage 2006;47:1550–73.
[89] Microwave assisted acid digestion of aqueous samples and extracts, USEPA, SW-846, 3015 A.
[90] ASTM, 2001 ASTM, 2001. D-4600-87: Standard test method for determination of benzene soluble particulate matter in workplace atmosphere.
[91] EPA method 3052: Microwave assisted acid digestion of siliceous and organically based matrices.
[92] Cachier H, Bremond MP, Buat-Menard P. Determination of atmospheric soot carbon with a simple thermal method. Tellus 1989;41B:379–90.
[93] Sharma M, Agarwal AK, Bharathi KVL. Characterization of Exhaust Particulates from Diesel Engine. Atmos Environ 2005;39(17):3023–8.
[94] Heywood JB. Fundamentals of Internal Combustion Engines. NY: McGraw Hill; 1988. p. 619.
[95] Wang Ya-Fen, Huang KL. Emissions of fuel metals content from a diesel vehicle engine. Atmos Environ 2003:4637–43.
[96] Volkswagen. Unregulated Motor Vehicle Exhaust Gas Components. Volkswagen AG, Research and Development (Physico-Chemical Metrology). Project Coordinator: Dr. K. H. Lies. 3180 Wolfsburg 1, F.R. Germany; 1989.
[97] California Environmental Protection Agency (CAL EPA). Part B: Health Risk Assessment for Diesel Exhaust, Proposed Identification of Diesel Exhaust as a Toxic Air Contaminant. Office of Environmental Health Hazard Assessment (OHEEA); 1998.
[98] ASTM D-4600-87: Standard Test Method for Determination of Benzene Soluble Particulate Matter in Workplace Atmospheres; 2001.
[99] Hinds WC. Aerosol Technology, Properties, Behavior and Measurement of Airborne Particles. 2nd edn. New York: John Wiley and Sons; 1999 [page 147, Table 7.6].
[100] Ning Z, Cheung CS, Liu SX. Experimental investigation of the effect of exhaust gas cooling on diesel particulate. J Aerosol Sci 2004;35:333–45.
[101] Dwivedi D, Agarwal AK, Sharma M. Particulate emission characterization of a biodiesel vs diesel fuelled compression ignition transport engine: a comparative study. Atmos Environ 2006;40(29):5586–95.
[102] El-Shobokshy MS. A preliminary analysis of the Inhalable particulate lead in the ambient atmosphere of the city of Riyadh, Saudi Arabia. Atmos Environ 1984;18(10):2125–30.
[103] Sharp CA. Emissions and Lubricity Evaluation of Rapeseed Derived Biodiesel Fuels. San Antonio, TX: Southwest Research Institute; 1996.
[104] Yehliu Kuen, André Boehman L, Armas Octavio. Emissions from different alternative diesel fuels operating with single and split fuel injection. Fuel 2010;89:423–37.
[105] Armas Octavio, Yehliu Kuen, André Boehman L. Effect of alternative fuels on exhaust emissions during diesel engine operation with matched combustion phasing. Fuel 2010;89:438–56.
[106] Luigi TB, Battistelli CL, Luigi C, Riccardo C, De CB, Laura LA, et al. Emission comparison of urban bus engine fueled with diesel oil and biodiesel blend. Sci Total Environ 2004;327:147–62.
[107] Mustafa C, Garpen HJV. Comparison of engine performance and ignition for petroleum diesel fuel, yellow grease biodiesel, and soy bean oil biodiesel. In: ASAE 0160050. 2001.
[108] Finch GL. Effects of Subchronic Inhalation Exposure of Rats to Emissions from Diesel Engine Burning Soybean Oil-Derived Biodiesel Fuel. Inhal Toxicol 2002;14:1017–48.